Four- and Five-Body Final States from 6.7-GeV/c π^-p Interactions*

S. MIYASHITA, J. VON KROGH, J. B. KOPELMAN, AND L. MARSHALL LIBBY
University of Colorado, Boulder, Colorado 80302
(Received 15 September 1969)

We have analyzed approximately 9000 four-prong events produced by π^-p interactions at 6.7 GeV/c. All the effective-mass distributions from final states $\pi^-\pi^-\pi^+p$, $\pi^-\pi^-\pi^+\pi^0p$, and $\pi^-\pi^-\pi^+\pi^+n$ are presented, as well as cross sections. Resonances in each final state amount to more than 50% of total events, dominated by ρ mesons and $\Delta(1236)$ baryons. Three-pion mass distributions show strong signals in the A-meson region in all three final states, but only a modest enhancement is observed in the R-meson region. We rule out J^P of 0^- and 2^+ for the $A_{1.5}$. A similar analysis for the A_1 is consistent with 1^+. In the $\pi\rho$ and $\pi\eta$ mass distributions no evidence for A_2 structure is seen. Low-mass enhancements in four-pion mass distributions appear in the region of the B meson and the $\rho(1700)$ meson. There is also possibly some evidence for $f'\to 4\pi$. Higher-mass nucleon isobars are found to be closely associated with $\Delta(1236)$ production. There is no significant production of quasi-two-body final states.

I. INTRODUCTION

A LARGE number of studies[1–22] of multipion final states in π^-p interactions have been made at a wide range of energies. Most of these have been at beam momenta below 6 GeV/c; however, recently several experiments[23] have been performed up to a momentum of 20 GeV/c. Much attention has been given to the four- and five-body final-state interactions

$$(1)\quad \pi^-p\to\pi^-\pi^-\pi^+p,$$
$$(2)\quad \pi^-p\to\pi^-\pi^-\pi^+p\pi^0,$$
$$(3)\quad \pi^-p\to\pi^-\pi^-\pi^+\pi^+n.$$

The characteristic features of these reactions can be summarized as follows:

(a) The cross sections rise from threshold to their maximum at a beam momentum of about 4 ± 1 GeV/c (see Table I). At higher momenta they gradually decrease, staying relatively flat for a considerable momentum range. In this region the cross-section ratio for reactions (2) and (3) is approximately equal to 1.7, the value predicted from isospin considerations.[24]

(b) At low energies, the statistical model seems to describe the interactions adequately. At higher energies a large increase in peripherality is noted,[25] indicating that the dynamics of the interaction are possibly dominated by fewer OPE-type (one-pion-exchange-type) diagrams. At a given pion momentum, final state (1) is considerably more peripheral than (2) and (3). Again this difference must be due to the dynamics, since the energy available to the particles in (1) differs very little from that available in (2) and (3).

(c) Major resonances produced in all three final states are the ρ meson and the Δ baryon. Reaction (1) is mediated by about equal amounts of ρ and $\Delta(1236)$ throughout a considerable energy range with, however, very little evidence for quasi-two-body production. Resonance production in final states (2) and (3) differs from that in (1) in that at lower energies there is significant production of $\Delta(1236)$ but an almost com-

TABLE I. Partial cross sections (mb).

Beam momentum (GeV/c)	Final state (1)	(2)	(3)
3.0	1.80	1.58	0.7
3.2	1.91±0.08	1.86±0.08	0.89±0.04
4.2	1.92±0.10	2.18±0.11	1.16±0.06
6.7	1.3 ±0.2	1.72±0.2	1.17±0.1
8.0	1.27		
10.0	1.01±0.21	1.77±0.35	1.03±0.24
13.0	1.14±0.15		
16.0	1.08±0.12		
20.0	0.89±0.08		

* Supported by the U. S. Atomic Energy Commission, under Contract No. AT-(11-1) 1537.
[1] See Refs. 2–22. π^+p data are not included.
[2] Saclay-Orsay-Bari-Bologna Collaboration, Nuovo Cimento **29**, 515 (1963).
[3] R. Christian *et al.*, Phys. Rev. **143**, 1105 (1966).
[4] D. D. Carmony, F. Grard, R. T. Van de Walle, and N. H. Xuong, in *Proceedings of the International Conference on High-Energy Physics*, edited by J. Prentki (CERN, Geneva, 1962).
[5] P. H. Satterblom, W. D. Walker, and A. R. Erwin, Phys. Rev. **134**, B207 (1964).
[6] J. Alitti *et al.*, Nuovo Cimento **35**, 1 (1965).
[7] A. W. Key *et al.*, Phys. Rev. **166**, 1430 (1968).
[8] S. V. Chung, O. I. Dahl, J. Kirz, and D. Miller, Phys. Rev. **165**, 1491 (1968).
[9] Aachen-Birmingham-Bonn-Hamburg-London(I. C.)-München Collaboration, Nuovo Cimento **31**, 485 (1964).
[10] G. Ascoli, H. B. Crawley, D. W. Montana, and A. Shapiro, Phys. Rev. Letters **20**, 1411 (1968).
[11] F. Bomse *et al.*, Phys. Rev. **162**, 1328 (1967).
[12] D. E. Alyea *et al.*, Phys. Rev. Letters **21**, 1421 (1968).
[13] J. von Krogh, S. Miyashita, J. B. Kopelman, and L. Libby, Phys. Letters **27B**, 254 (1968).
[14] N. M. Cason, Phys. Rev. **148**, 1282 (1966).
[15] T. F. Johnston *et al.*, Phys. Rev. Letters **20**, 1414 (1968).
[16] V. A. Belyakov *et al.*, Yadern. Fiz. **5**, 1232 (1967) [English transl.: Soviet J. Nucl. Phys. **5**, 880 (1967)].
[17] N. N. Biswas *et al.*, Phys. Rev. Letters **21**, 50 (1968).
[18] N. N. Biswas, I. Derado, N. Schmitz, and W. D. Shephard, Phys. Rev. **134**, B901 (1964).
[19] J. Ballam *et al.*, SLAC Report No. SLAC-PUB-480, 1968 (unpublished).
[20] C. Caso *et al.*, Nuovo Cimento **54A**, 983 (1968).
[21] J. Bartke and O. Czyzewski, Nucl. Phys. **B5**, 582 (1968).
[22] M. L. Ioffredo *et al.*, Phys. Rev. Letters **21**, 1212 (1968).
[23] See Refs. 10, 12, and 19. See also Ref. 68.
[24] J. Shapiro, Nuovo Cimento Suppl. **18**, 40 (1960).
[25] O. Czyzewski, in *Proceedings of the Fourteenth International Conference on High-Energy Physics, Vienna, 1968*, edited by J. Prentki and J. Steinberger (CERN, Geneva, 1968), p. 367.

TABLE II. ρ^0 production cross section (μb).

Beam momentum (GeV/c)	Final state (1)	(2)	(3)
3.0	720±70	very small	very small
3.2	480±70	very small	65
4.2	520±70	small	70
6.7	571±144	260±67	410±93
8.0	560±40		
10.0	700±100	270±120	190±70

TABLE III. $\Delta(1236)$ production cross section (μb).

Beam momentum (GeV/c)	Final state (1) (Δ^{++})	(2) (Δ^{++})	(3) (Δ^-)
2.7			480±80
3.0	730±70	470±90	410±100
3.2	590±70	320±80	300±50
4.2	590±70	335±65	340±50
6.7	300±80	350±100	245±80
8.0	320±50		
10.0	100±40		

plete absence of bosons. Boson production increases with higher energies, even though the relative dominance of nucleon isobars does not change.

(d) Higher-mass resonances are closely associated with low-lying states, undergoing cascade-type decays. There is little indication of higher states decaying directly into stable particles.

In this experiment, the above reactions were studied at a beam momentum of 6.7 GeV/c. 100 000 exposures taken in the 30-in. hydrogen bubble chamber at Argonne National Laboratory were analyzed using the Berkeley programs TVGP and SQUAW. The events were selected requiring consistency between kinematical-fit information and ionization checks. Approximately 10% of the events failed the reconstruction program and were remeasured. A complete roll was measured twice in order to test the reproducibility of the experiment. In 96% of the events the same results were obtained, indicating a high level of confidence in the measurement and fitting procedures. About 25 000 four-prong events were measured and classified into reactions (1), 3633 events; (2), 3863 events; and (3), 2618 events.

II. FINAL STATE $\pi^-\pi^-\pi^+p$

A. General Features

This final state is dominated by the production of two resonances, the ρ meson and the $\Delta(1236)$ baryon[26] (see Fig. 1). The respective cross sections are given in Tables II and III. The corresponding uncertainties include statistical errors, scanning errors, and the effect of beam length, as well as uncertainties in fitting the mass spectra and in the choice of background for these fits. Simple phase space does not describe this final state very well (see Fig. 1), because there is a high degree of peripherality, as illustrated in the angular distributions of the outgoing particles (Fig. 2). Peripheralization of phase space yields improvement in fitting the background but has not been necessary for our analysis, as will be demonstrated.

$\Delta(1236)$ production is observed in both the $M(\pi^+p)$ and the $M(\pi^-p)$ distributions [Figs. 1(c) and 1(d)]. Whereas the π^+p mass does not show other resonances, there is a second enhancement in the π^-p mass between 1500 and 1700 MeV. From its absence in the π^+p channel, this enhancement must appear only in the $I=\frac{1}{2}$ state. Baryon resonances in this mass region are quite closely spaced, and the peaking could be explained by some combination of the following: $N(1518)$, $N(1550)$, $N(1680)$, $N(1688)$, and $N(1710)$.

Production of higher resonances is observed in the $\pi^-\pi^-\pi^+$ as well as the $\pi^-\pi^+p$ histograms [Figs. 1(e) and 1(f)]. In the three-pion mass spectrum there are enhancements around 1300 and 1650 MeV, which can be due to production of A_2 and A_3 mesons, although the latter is not statistically significant in this uncut mass distribution (see Table IV). Suitable cuts enhance these peaks, and A mesons are discussed in detail in Sec. II B. A detailed analysis of higher baryon resonances in this final state, as well as in final states (2) and (3), has been made elsewhere.[27]

TABLE IV. A-meson production cross section (μb).[a]

Beam momentum (GeV/c)	Final state (1) A_1	$A_{1.5}$	A_2	Final state (3) A_1	A_2
3.0	30 ±23		130±34		
3.2	140 ±23		150±50		
4.2	160 ±60		175±45		
6.7	19 ±19	44±20	34±14	58±22	37±13
8.0	0.2± 0.2	15±5	42±12		
16.0	250±50		180±60		

[26] Fitting the mass spectra in Fig. 1, we obtain the parameters: ρ, ($M=767\pm3$ MeV, $\Gamma=135\pm11$ MeV); Δ^{++}, ($M=1211\pm3$ MeV, $\Gamma=93\pm8$ MeV). Events forming the $\Delta(1236)$ are not distributed uniformly in $\cos\alpha$, but form the forward direction (here α is the angle between the incoming p and the outgoing Δ, evaluated in the over-all center-of-mass system). The same holds true for ρ^0 and f^0 production. A reasonable way to cut on these resonances would then be to cut in both mass and in $\cos\alpha$. Therefore, unless specified differently, the following cuts are used:

ρ^0 cut: $0.66 < M(\pi^-\pi^+) < 0.86$ GeV, $0.7 < \cos(\pi^-,\pi^-\pi^+) < 1.0$;
f^0 cut: $1.16 < M(\pi^-\pi^+) < 1.36$ GeV, $0.7 < \cos(\pi^-,\pi^-\pi^+) < 1.0$;
Δ^{++} cut: $1.136 < M(\pi^+p) < 1.336$ GeV, $0.7 < \cos(p,\pi^+p) < 1.0$.

[a] Caution should be used when comparing the cross sections in Table IV. The question of background is not resolved and is treated differently by different experimenters. Some of the large cross sections for A_1 production are possible because no kinematic background is assumed.

[27] S. Miyashita, J. von Krogh, J. B. Kopelman, and L. M. Libby, Nuovo Cimento (to be published).

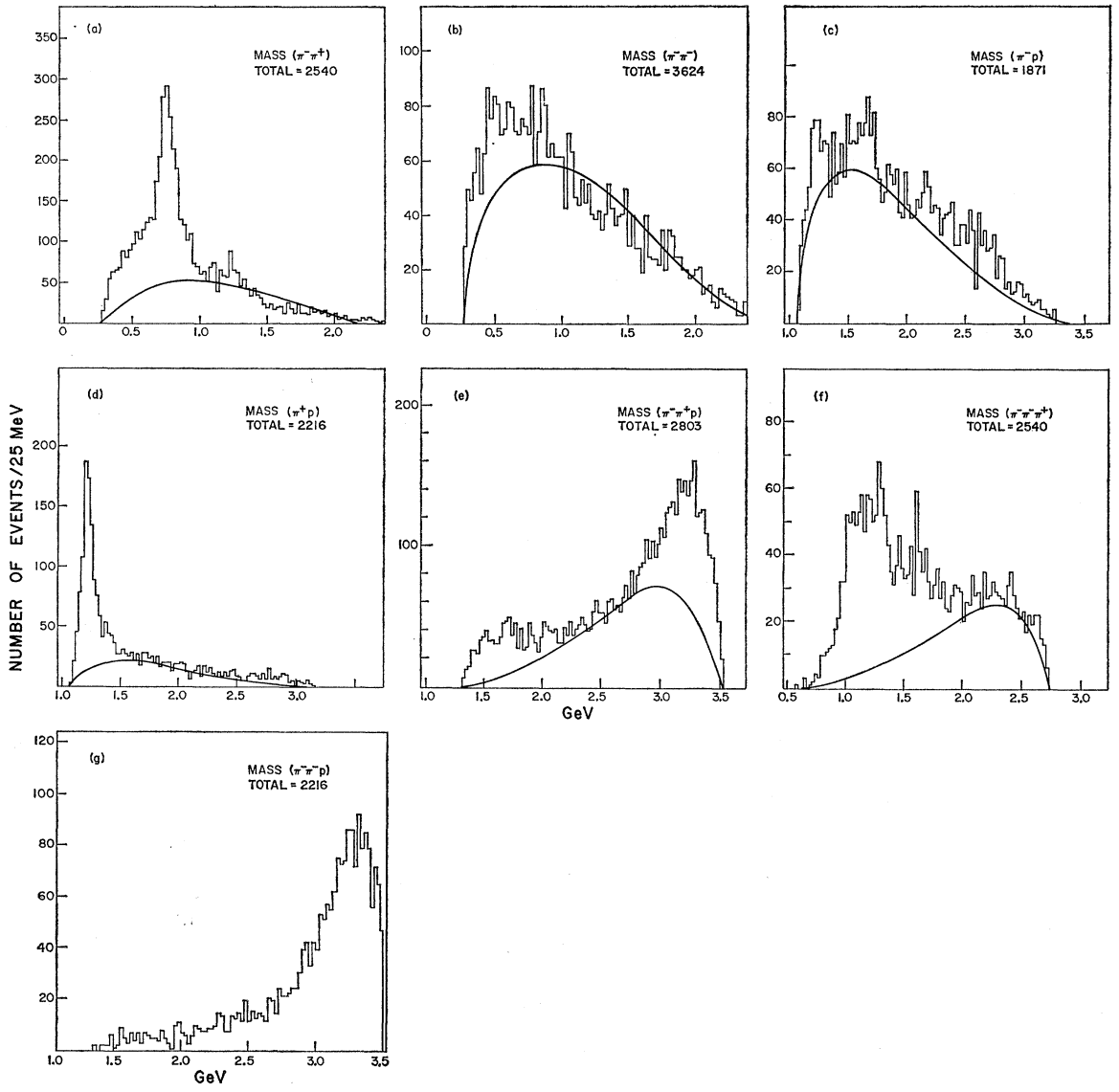

FIG. 1. Invariant-mass distributions for the final state (1). Reflections from dominant resonances are removed (Ref. 93). The solid curves represent phase space.

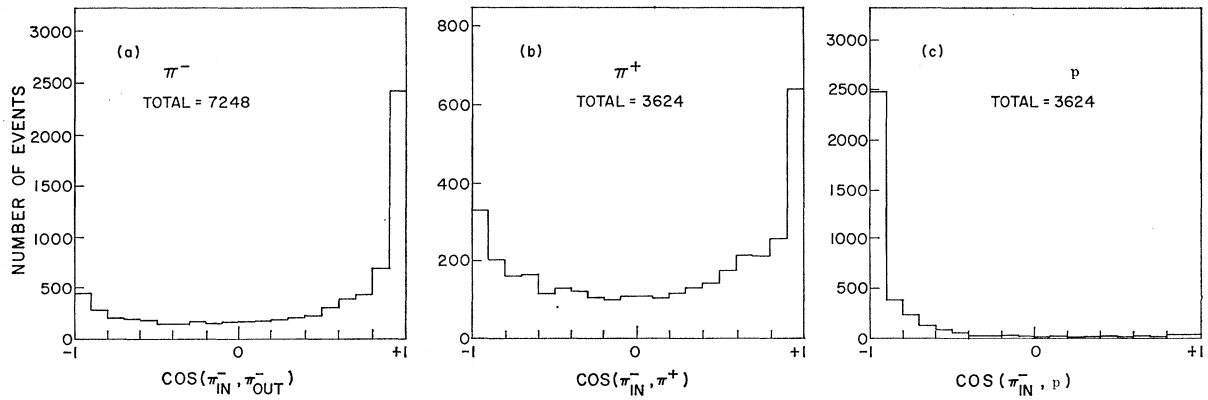

FIG. 2. Angular distribution for outgoing particles in the over-all center-of-mass system from the final state (1).

B. Analysis of $\pi^-\pi^-\pi^+$ Mass Spectrum

From Fig. 1(f) we see that the 3π mass spectrum from 2450 events contains two regions of interest, an enhancement between 1.0 and 1.4 GeV, and a narrower peak at 1.6 GeV superimposed on the nonresonant background. The statistical significance of the second peak is somewhat improved by requiring a dipion mass to be in the f^0 region, and this is discussed in the last part of this section.

1. $\pi\rho$ Mass Spectrum

Before investigating the mass region of the A mesons, we review what is known of the $\pi\rho$ mass spectrum from other experiments. Two resonances are normally observed, with masses of 1080 and 1300 MeV, called the A_1 and A_2 mesons, respectively. Even though it is generally agreed that the spin J and parity P of the A_1 is $J^P=1^+$, there is disagreement on the question of whether the A_1 actually exists. Some experiments[28–30] report two distinct peaks; others at similar energies see much less evidence for the A_1.[31,32] A compilation of data[28] from 2.75 to 4.2 GeV/c shows that peaks at 1080 MeV are usually much smaller than the A_2 at 1320 MeV. The best evidence here for a real A_1 meson is given in the data by the Aachen-Berlin-CERN collaboration,[33] but the other experiments do not seem to resolve the A_1 and A_2 very clearly.[34–38] In a compilation over all energies,[39] the A_1 peak disappears almost completely. Even though there is considerable evidence against a resonance interpretation of the A_1, there is one strong feature which speaks for it. Production of $A_1^0 \to \pi^\pm\rho^\mp$ has recently been observed in two experiments.[40,41] As an $I=1$ resonance, the A_1^0 should decay into $\rho^-\pi^+$, $\rho^+\pi^-$, and $\rho^0\pi^0$ in the ratios 1:1:0 and both experiments give agreement with this prediction. We should note that both of these reports are for K^--nucleon interactions. So far, no clear evidence for A_1^0 production has been seen in π^--nucleon interactions. It is difficult to see why there should be more A_1^0 in K^-p interactions than in π^-p interactions.

Even though the existence of the A_2 is well established, there are complications. The accepted value of the spin and parity for the A_2 is $J^P=2^+$.[31,42,43] From the variation of cross section with incident momentum for two-body or quasi-two-body reaction, however, there is some evidence for a superposition of the A_2 and a $J^P=2^-$ (or 1^+) 3π resonance.[44] The newest data from the missing-mass spectrometer in CERN[45,46] show a splitting of the A_2 into two narrow peaks. This experiment has been repeated with different apparatus and a different method[47] (the A_2 being produced at minimum momentum transfer), with the same result. For the most part, mass resolution of bubble-chamber experiments is insufficient for observation of this effect; only recently one such experiment[48] has confirmed the splitting. Additional bubble-chamber data show[49] a $\rho^-\pi^-$ peak at 1310 MeV with isospin $I=2$. A knowledge of the cross section for A_2^- production as well as for $(\rho^-\pi^-)$ production, together with isospin considerations [using $I=2$ for the $\rho^-\pi^-(1310)$], enables us to conclude that the cross section for its singly charged state should be almost negligible compared to the cross section for A_2 production.[44] Hence it will not be an important background consideration when studying the A_2.

There are some indications for an additional narrow resonance with a mass of 1170–1190 MeV of width about 20–40 MeV, for which the name $A_{1.5}$ has been used.[14,50–53]

---

[28] An excellent review with plots shown from most experiments is given by G. Goldhaber, in *Proceedings of the Thirteenth International Conference on High-Energy Physics, Berkeley, 1966* (University of California Press, Berkeley, 1967), p. 120; G. Goldhaber *et al.*, Phys. Rev. Letters **12**, 336 (1964).

[29] Aachen-Berlin-Birmingham-Bonn-Hamburg-London (I. C.)-München Collaboration, Phys. Letters **10**, 226 (1964).

[30] B. C. Shen, G. Goldhaber, S. Goldhaber, and J. A. Kadyk, Phys. Rev. Letters **15**, 731 (1965).

[31] G. Benson *et al.*, Phys. Rev. Letters **16**, 1177 (1966).

[32] S. U. Chung *et al.*, Phys. Rev. Letters **18**, 100 (1967).

[33] Aachen-Berlin-CERN Collaboration, Phys. Letters **22**, 112 (1966). The ABC experiment separates A_1 and A_2 beautifully. In their newest data they have almost doubled their statistics and the A_1 and A_2 are not resolved any more. This is not because their resolution has deteriorated (they know from their ω^0 width, that it has not), but is just a result of statistical fluctuations. See Ref. 66, p. 17.

[34] V. E. Barnes *et al.*, Phys. Rev. Letters **16**, 41 (1966).

[35] P. Slattery, H. Kraybill, B. Forman, and T. Ferbel, Nuovo Cimento **50A**, 4541 (1967).

[36] A. Garfinkel *et al.* (see Ref. 28).

[37] Bari-Bologna-Firenze-Orsay Collaboration, Phys. Letters **25B**, 53 (1967).

[38] J. Ballam *et al.*, Phys. Rev. Letters **21**, 934 (1968).

[39] T. Ferbel, Phys. Letters **21**, 111 (1966).

[40] R. E. Juhala, R. A. Leacock, J. I. Rhode, J. B. Kopelman, L. M. Libby, and E. Urvater, Phys. Rev. Letters **19**, 1355 (1967).

[41] W. Hoogland, J. C. Kluyver, and A. G. Tenner, in *Proceedings of the Heidelberg International Conference on Elementary Particles*, edited by H. Filthuth (North-Holland Publishing Co., Amsterdam, New York, 1968); J. C. Berlinghieri, M. S. Farber, T. Ferbel, R. Holmes, P. F. Slattery, S. Stone, and H. Yuta, Phys. Rev. Letters **23**, 42 (1969).

[42] S. U. Chung *et al.*, Phys. Rev. Letters **12**, 621 (1964).

[43] C. Baltay, L. Kirsch, H. H. Kung, N. Yeh, and M. Rabin, Phys. Letters **25B**, 160 (1967).

[44] D. R. O. Morrison, Phys. Letters **25B**, 238 (1967).

[45] G. Chikovani *et al.*, Phys. Letters **25B**, 44 (1967).

[46] G. Chikovani, R. Baud, H. Benz, B. Bosniakovic, G. Damgaard, M. Focacci, W. Kienzle, M. Klanner, C. Lechanoine, M. Martin, C. Nef, P. Schubelin, and A. Weitsch, in *Proceedings of an Informal Meeting on Experimental Meson Spectroscopy, Philadelphia, 1968* (W. A. Benjamin, Inc., New York, 1968).

[47] H. Benz, G. E. Chiovani, G. Damgaard, M. N. Focacci, W. Kienzle, C. Lechanoine, M. Martin, C. Nef, P. Schubelin, R. Band, B. Bosniakovic, J. Cofferon, R. Klanner, and A. Weitsch, Phys. Letters **28B**, 233 (1968).

[48] D. Crennell, U. Karshon, K. Lai, J. Scarr, and I. Skillicorn, Phys. Rev. Letters **20**, 1318 (1968).

[49] R. Vanderhagen *et al.*, Phys. Letters **24B**, 493 (1967).

[50] G. Ascoli, H. Crawley, U. Kruse, D. Mortara, E. Schafer, A. Shapiro, and B. Terreault, Phys. Rev. Letters **21**, 113 (1968).

[51] N. Cason, J. Lamsa, N. Biswas, I. Derado, T. Groves, V. Kenney, J. Poirier, and W. Shephard, Phys. Rev. Letters **18**, 880 (1967).

[52] I. Butterworth, Rutherford High-Energy Laboratory Report No. HEP/MISC/6, 1969, p. 43 (unpublished). See also p. 24 of Ref. 66.

[53] J. von Krogh, J. Kopelman, and L. Libby, in *Lectures in Theoretical Physics* (Gordon and Breach, Science Publishers, Inc., New York, 1968), Vol. 10B.

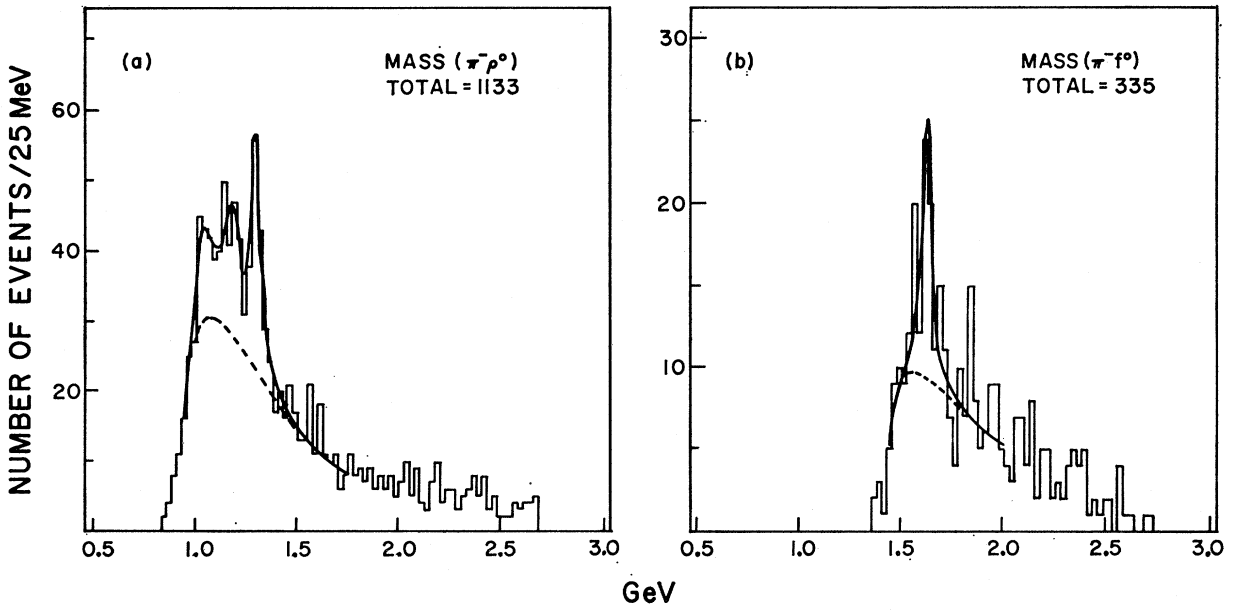

FIG. 3. (a) $M(\pi^-\rho^0)$ distribution. (b) $M(\pi^-f^0)$ distribution.

It is quite possible that most previous experiments did not have sufficient mass resolution to distinguish between the A_1 and the $A_{1.5}$.[54] This might explain the large variations in the features of A_1 production in many experiments. Both the A_1 and the $A_{1.5}$ are produced with small four-momentum transfer squared, explaining why neither one is observed by the missing-mass spectrometer where the data are taken at fixed Δ^2.

Figure 3(a) shows a histogram for mass $M(\pi^-\rho^0)$, with $\Delta^{++}(1236)$ excluded. The A_2 at 1300 MeV has been enhanced; a small peak has appeared in the A_1 region between 1000 and 1100 MeV, and between these there is some structure which could be associated with the $A_{1.5}$. It is well known that the low-mass enhancement in the $\pi\rho$ mass can be caused not only by real resonance production, but also—at least in part—by peripheral OPE diagrams (Deck mechanism).[50–56] In fact, a Regge-exchange model[57] favors a kinematical interpretation of this enhancement. The Deck effect, indeed, accounts for a large part of the low-mass enhancement, but fails to reproduce a narrow peak [see the dashed line in Fig. 3(a)]. With this background, which we will discuss more in detail in the following, we tested the other possibility that one big peak is produced together with the A_2 signal. The obtained mass and width ($M\approx1170$ MeV, $\Gamma\sim200$ MeV) seem to be incompatible with other experiments for resonance interpretation. However, if we take an OPE model, we get a much better fit to the data with three peaks, A_1, $A_{1.5}$, and A_3, and we get resonance parameters consistent with other experiments analyzed by similar methods.

We present our analysis based on an OPE model. The simplest OPE diagrams are (a) with π exchange, where the ρ is produced at the meson vertex, and (b) with ρ exchange, where the ρ is scattered at the baryon vertex. In both cases, diffraction scattering at the baryon vertex has the effect that the π and ρ mesons come off together in the c.m. system and simulate a low-mass $\pi\rho$ resonance. We have discussed this background question elsewhere in detail.[53] From studies of $\Delta^2(\pi^-,\pi^-)$, $\Delta^2(\pi^-,\rho^0)$, and Treiman-Yang angular distributions, we conclude that a ratio (π exchange)/(ρ exchange) = 53/47 is most consistent with our data as an estimate for kinematic background.

Numerous calculations have been made for the effect resulting from diagram (a) with π exchange,[55,56,58] and Cason *et al.*[58] have made calculations for ρ exchange (b). We have used the sum of both diagrams in the ratio 53/47 as background for a Breit-Wigner fit.

Usually one attempts separation of the A_1 and A_2 by making four-momentum-transfer cuts at 0.1–0.5 $(\text{GeV}/c)^2$. In this way one hopes to eliminate most of the Deck background, which stems from high peripherality. These attempts are "artificial," in that small $\Delta^2(p_{\text{in}},p_{\text{out}})$ kinematically relate to small $(\pi\rho)$ masses in our four-body interaction. Consequently, we will refrain from making such Δ^2 cuts.

[54] Compare, e.g., the data by U. E. Kruse *et al.* in plots 7-35 and 7-37 of Ref. 28.

[55] R. T. Deck, Phys. Rev. Letters **16**, 169 (1964).

[56] U. Maor and T. A. O'Halloran, Jr., Phys. Letters **15**, 281 (1965).

[57] The distribution could be explained without production of A_1 only if we choose about 100% diagram (b) (ρ exchange). See also E. L. Berger [Phys. Rev. **166**, 1525 (1968)], who reproduced almost all of the A_1 enhancement by a Regge-pole-exchange model.

[58] See Ref. 51.

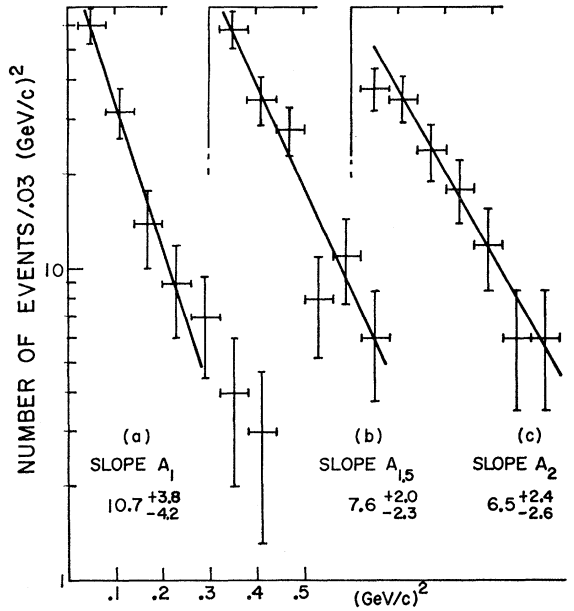

FIG. 4. Distributions in four-momentum transfer squared $\Delta^2(\pi_{in}^-,\pi^-\rho^0)$: (a) A_1 region, $1010<M(\pi^-\rho^0)<1100$ MeV; (b) $A_{1.5}$ region, $1140<M(\pi^-\rho^0)<1240$ MeV; (c) A_2 region, $1250<M(\pi^-\rho^0)<1350$ MeV.

The distribution obtained in the way discussed above, and shown as the lower curve in Fig. 3(a), peaks at ~1100 MeV. If the high-mass tail of the curve is normalized to our experimental distribution, the peak itself is not steep enough to explain the distribution without assuming production of a real A_1.[57] We have made a fit with three Breit-Wigner profiles[59] superimposed on the kinematic background with best parameters (in MeV) as follows: A_1, ($M=1136\pm9$, $\Gamma=44\pm42$); $A_{1.5}$, ($M=1174\pm17$, $\Gamma=111\pm63$); and A_2, ($M=1307\pm5$, $\Gamma=43\pm19$).

In the simplest diagram for production of three-pion–boson resonances, the Δ^2 distribution for production of resonances fits well to an exponential form $e^{-a\Delta^2}$.[60] We have investigated each of the A mesons with respect to this and give in Figs. 4(a)–4(c) the relevant distributions. The slopes are $a=10.7_{-4.2}^{+3.8}$ $(\mathrm{GeV}/c)^{-2}$ for the A_1, $a=7.6_{-2.3}^{+2.0}$ $(\mathrm{GeV}/c)^{-2}$ for the $A_{1.5}$, and $a=6.5_{-2.6}^{+2.4}$ $(\mathrm{GeV}/c)^{-2}$ for the A_2.

We quote values of a without background subtraction, since the Δ^2 behavior of the background is not known *a priori*.

The A_2 has been observed to be split into two peaks in several experiments.[47,48,61] In principle, our mass resolution[62] of 5–10 MeV is small enough to show splitting, and we have studied this, but find no significant effect.

(*a*) *Spin and parity* J^P. We use the Berman-Jacob[63] analysis for the decay of a boson into three pions and investigate the distribution of $\cos\alpha$, where α is the polar angle between normal of the boson decay plane and incident π^- direction evaluated in the boson rest frame. Our approach is to compare the distribution in $\cos\alpha$ with that obtained by the theoretical calculation for a given J^P. The theoretical distributions[63] are shown in Table V. When deriving the above angular distributions, we have made several assumptions. Since not all of these are necessary, in principle, we state them here. We have used a symmetry property of the density matrix elements, which follows from parity conservation in the production process[46–64] $\rho_{-m,-m'}=(-1)^{m-m'}\rho_{mm'}$. Secondly, we assume that the A is produced via ρ^0 exchange. Angular momentum conservation at the meson production vertex then requires that certain matrix elements vanish identically. This assumption makes the analysis somewhat model-dependent. The decisive factor here is the limited statistics of our data sample, which makes fits to distributions with more than three free parameters meaningless.

(*b*) *Spin and parity of* A_1. The A_1 peak, extending from 1.0 to 1.1 GeV, contains about 65% background. which has to be subtracted. Unfortunately, no suitable control regions for background estimation exist for the A_1, since the $A_{1.5}$ is directly adjacent to it at higher mass and the mass region below it does not contain enough events. From theoretical considerations[65] we expect a spin-parity assignment of 1^+ for a kinematic enhancement of a π-ρ combination. This information is not sufficient to correct for background, however, since the 1^+ distribution contains the parameter ρ_{11}, which is not known. Figure 5(a) shows the decay angular distribution for the A_1 including background.

Without making any formal fits, we can say that it shows the characteristics of a 1^+ or 1^- distribution. These distributions are very similar in shape, identical for $\rho_{11}=0$. If we assume no interference between resonance and background, Fig. 5(a) can be interpreted as a superposition of a 1^+ background and a resonance having 1^+ or 1^- as its spin-parity assignment.

(*c*) *Spin and parity of* $A_{1.5}$ About 70% of the events in the $A_{1.5}$ region, taken from 1.125 to 1.25 GeV, is background. Most of this background is caused by the wide kinematic enhancement, which peaks at 1.1 GeV. Neglecting contributions of the tails of the adjacent resonances A_1 and A_2, and realizing the essentially

[59] Throughout this paper we use the classical Breit-Wigner shape $(\Gamma/2)^2/[(m-M)^2+(\Gamma/2)^2]$.

[60] L. di Lella, in *Proceedings of the Heidelberg International Conference on Elementary Particles, Heidelberg, 1967*, edited by H. Filthuth (North-Holland Publishing Co., Amsterdam, 1968), p. 157.

[61] Anguilar-Benitez *et al.*, in *Proceedings of the Fourteenth International Conference on High-Energy Physics, Vienna, 1968*, edited by J. Prentki and J. Steinberger (CERN, Geneva, 1968), p. 111.

[62] We have studied the resolution by making multiple measurements of the same event. The resolution was obtained from the spread of the (3π) mass after the measurements were fitted by the regular program.

[63] S. Berman and M. Jacob, Phys. Rev. **139B**, 1023 (1965).

[64] K. Gottfried and J. D. Jackson, Nuovo Cimento **33**, 309 (1964); Phys. Letters **8**, 144 (1964).

[65] L. Stodolsky, Phys. Rev. Letters **18**, 973 (1967).

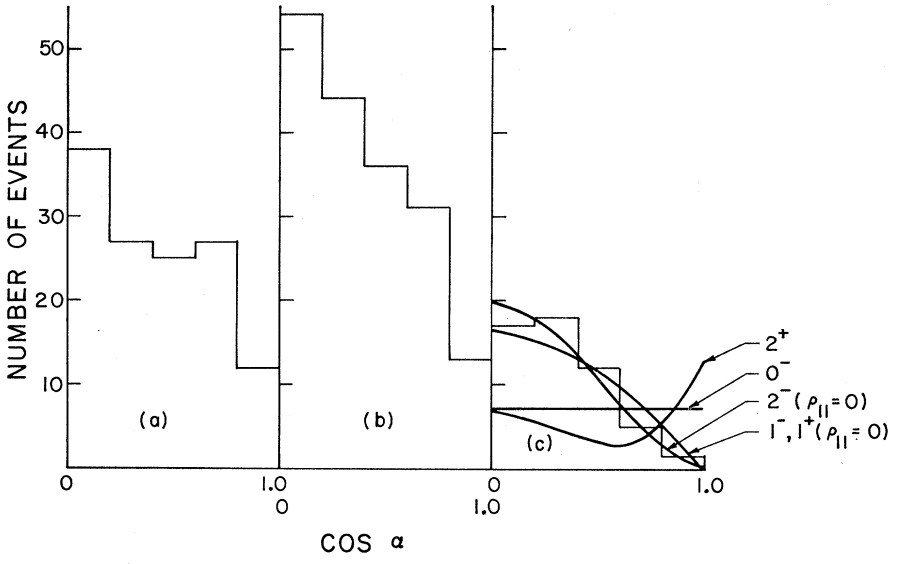

FIG. 5. Angular distributions of decay normal for $A_{1.5}$: (a) A_1 region, 1060–1140 MeV; (b) $A_{1.5}$, uncorrected, 1140–1240 MeV; (c) $A_{1.5}$, corrected, 70% background subtracted.

similar angular behavior of A_1 and a kinematic enhancement, we can use the A_1 region for estimation of the background under the $A_{1.5}$. The uncorrected decay angular distribution is shown in Fig. 5(b) and the distribution with background subtraction (again we assume noninterference) in Fig. 5(c). The amount of background subtracted has been determined from the Breit-Wigner fit discussed earlier. The smooth curves are fits to the theoretical distributions for different spin-parity assignments. The levels of confidence determined by our data are shown in Table V. The resultant angular distribution is very insensitive to variations in the amount of background subtracted. There are only 50 events remaining after subtraction of the background, too few to allow a definite determination of quantum numbers, but the assignments 0^- and 2^+ seem to be less likely.

(*d*) *Spin and parity of* A_2. A similar spin-parity analysis for the A_2 is shown in Figs. 6(a)–6(c). We have chosen the distributions from 1.25 to 1.35 and from 1.35 to 1.55 GeV, respectively, as a resonance region for the A_2 and a suitable control region. The results are given in Table V. Our data are consistent with spin-parity of 2^+ as previously reported,[9] but, with only 60 events remaining, we cannot exclude 1^+. Chung *et al.*[8] exclude the assignments 1^+ and 2^- after correcting for background and making Δ^2 cuts to eliminate Deck background. As Butterworth[66] points out, there are dangers in such Δ^2 cuts, since diffractive processes are the hypothetical origin of the 2^- or 1^+ meson. The correct way of studying this is to see whether or not fits to the $\pi\rho$ Dalitz plot through the A_2 region show the $1^+/2^-$ background peaking as well as the 2^+ matrix element. This is difficult and no one has yet succeeded.[66]

(*e*) *Branching ratios of A mesons.* From Fig. 1(f) and 3(a), we see that we have to consider two modes: $A \to \pi^-\pi^-\pi^+$ and $A^- \to \pi^-\rho^0$. The fact that the two ρ bands in a decay Dalitz plot overlap plus the effect of background from direct (3π) decay and kinematic effects make it impossible to obtain reliable information on the decay modes from a study of the mass distributions $M(\pi\rho)$ and $M(3\pi)$ alone. Instead, a complete analysis of the whole Dalitz plot, dependent on spin-parity assignments for the A, is necessary.[67] The complete analysis requires considerably more events than we have and we must be content with the information from the effective-mass plot. Comparing the cross sections for resonance production in the mass histograms M(all 3π) and $M(\pi\rho)$, we see little evidence for direct 3π decay. In the regions of the A_1 ($M = 1050 \pm 50$ MeV), $A_{1.5}$ ($M = 1190 \pm 60$ MeV), and the A_2 boson (1300 ± 50 MeV) we find $R = (A^- \to \pi^-\rho^0)/(A^- \to$ all $\pi^-\pi^-\pi^+) \geq 82\%$ for A_1, $\geq 83\%$ for $A_{1.5}$, and $\geq 75\%$ for A_2. The uncertainties in these ratios are approximately 50%.

TABLE V. Decay normal angular distributions for A mesons. ρ_{ij} are the elements of the spin density matrix for the A meson, and a and b are constants depending, in general, on the internal structure of the $\pi\rho$ system.

J^P	$dN/d(\cos\alpha)$	Level of confidence (%) $A_{1.5}$	A_2
0^-	a	10	55
1^+	$a(\sin^2\alpha - \rho_{11}(1-3\cos^2\alpha))$	90 ($\rho_{11}=0$)	80 ($\rho_{11}=0.6$)
1^-	$a\sin^2\alpha$	95	2
2^+	$a(\cos^2\alpha+\cos^2(2\alpha))$	2	95
2^-	$a(3\sin^4\alpha - 2\rho_{11}(1-5\cos^2\alpha) \times\sin^2\alpha)+b((1-3\cos^2\alpha)^2 -2\rho_{11}(1-12\cos^2\alpha+15\cos^4\alpha))$	95 ($\rho_{11}=0$)	40 ($\rho_{11}-1$)

[66] I. Butterworth, in *Proceedings of the Heidelberg International Conference on Elementary Particles*, edited by H. Filthuth (North-Holland Publishing Co., Amsterdam, 1968), p. 11.

[67] Aachen-Berlin-CERN Collaboration (J. Bartsch *et al.*), Nucl. Phys. **B7**, 345 (1968).

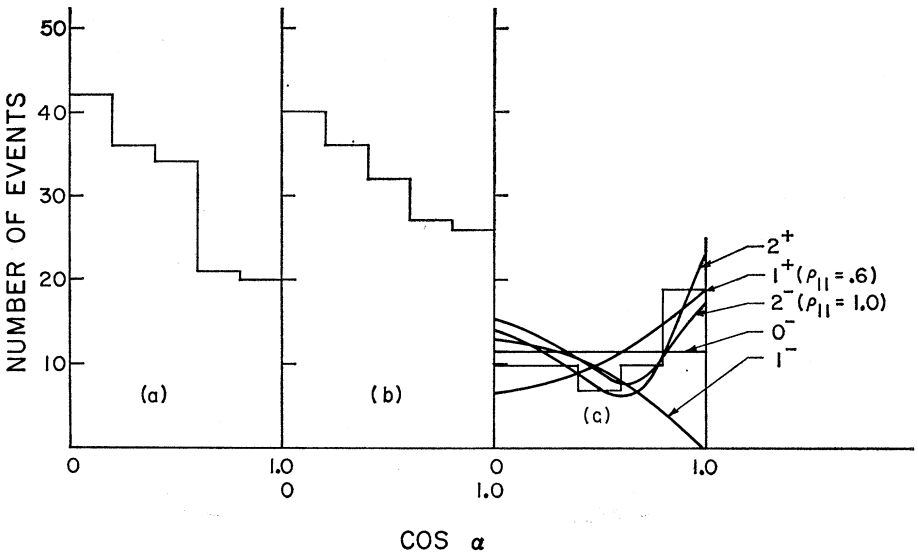

FIG. 6. Angular distributions of decay normal for A_2: (a) control region, 1350–1550 MeV; (b) A_2, uncorrected, 1250–1350 MeV; (c) A_2, corrected, 70% background subtracted.

2. π^--f^0 *Mass Spectrum*

The three-pion mass region 1.6–1.88 GeV, the so-called R region, studied both by missing-mass spectrometer and bubble-chamber techniques, is found to be extremely complex.[68] In Fig. 3(b) there is a peak between 1600 and 1700 MeV in the three-pion mass that can be associated with the A_3 or $\pi_A(1640)$ previously reported in the $(3\pi)^{\pm}$ mass.[67,51,69–74] Its mass and width from these experiments are $M=1648\pm10$ MeV [75] and $\Gamma=90\pm25$ MeV.[76] Most groups agree that it decays partially into $\pi^{\mp}f^0$ (indicating $I=1$) and that the enhancement almost disappears if required to contain a ρ^0. Spin-parity analysis[67] favors the abnormal series defined as $J^P=0^-$, 1^+, 2^-, etc. There is also indication of a 3π peak at a mass of 1651 MeV[77,78]; however, it is different from the A_3, since it seems to have the decay mode $\pi^0\rho^0$, suggesting $I=0$.

As in the case of the A_1 meson, a Deck calculation for the reaction $\pi^-p\to\pi^-f^0p$ predicts a wide enhancement in the π^-f^0 mass at about 1600 MeV.[67] In fact, no similar calculations can predict a peak narrow enough to explain the A_3 as a kinematic effect.

Our distribution of $M(\pi^-f^0)$ is in Fig. 3(b). We have made a fit to it using one Breit-Wigner peak plus kinematic background, taken from the ABC collaboration at 8 GeV/c,[67] and find the following parameters for the A_3: ($M=1633\pm12$ MeV, $\Gamma=37\pm24$ MeV).

There is a clear discrepancy in the values obtained for the width of the A_3 from bubble-chamber experiments ($\Gamma_{A_3}\sim100$ MeV) and from the CERN missing-mass spectrometer ($\Gamma_{A_3}<30$ MeV). This is a real discrepancy, since the mass resolution for both experimental techniques is certainly good enough (<30 MeV). In this experiment we observe a width of 37 MeV, 2.5 standard deviations away from the width typically measured in bubble-chamber experiments. We did not find any evidence for structure of the A_3.

For the slope of the Δ^2 distribution $e^{-a\Delta^2}$, we obtain $a=4.0_{-2.5}{}^{+2.8}$ (GeV/c)$^{-2}$. Again, we have not made any corrections for possible background. Rough estimates for the branching ratios for the A_3 decay are

$$(A_3\to\pi^-\rho^0)/(A_3\to\text{all }\pi^-\pi^-\pi^+)<17\%$$

and

$$(A_3\to\pi^-f^0)/(A_3\to\text{all }\pi^-\pi^-\pi^+)\geq51\%.$$

Uncertainties are at least of the order of 50%.

TABLE VI. Resonance production cross sections.[a]

Resonance	No. of events	Strength (%)
1. $\pi^-p\to\pi^-\pi^-\pi^+\pi^0p$		
ρ^-	680±130	18 ±4
ρ^0	580±120	15 ±3
ω^0	350±50	9 ±1
$\Delta^{++}(1236)$	780±100	20 ±3
$\Delta^+(1236)$	240±100	6 ±3
$\Delta^-(1236)$	130±60	3.4±1.6
ρ^-, ρ^0 associated	210±40	5.4±1
ρ^-, Δ^{++} associated	100±30	2.6±1
2. $\pi^-p\to\pi^-\pi^-\pi^+\pi^+n$		
ρ^0	920±160	35 ±6
$\Delta^-(1236)$	540±110	21 ±4
$\Delta^+(1236)$	200±80	8 ±3
ρ^0, ρ^0 associated	137±30	5.2±1
ρ^0, Δ^- associated	110±30	4.2±1
ρ^0, Δ^+ associated	80±20	3.1±1

[a] The cross section per event is 0.45 μb for both reactions (1) and (2). The table does not contain corrections for unseen decay modes.

[68] B. French, *Proceedings of the Fourteenth International Conference on High-Energy Physics, Vienna, 1968*, edited by J. Prentki and J. Steinberger (CERN, Geneva, 1968), p. 89.
[69] C. Baltay *et al.*, Phys. Rev. Letters **20**, 887 (1968).
[70] K. Boesebeck *et al.*, Nuclear. Phys. **B4**, 501 (1968).
[71] C. Caro *et al.*, Nuovo Cimento **54**, 983 (1968).
[72] I. A. Vetlitsky *et al.*, Phys. Letters **21**, 579 (1966).
[73] J. W. Lamsa *et al.*, Phys. Rev. **166**, 1995 (1968).
[74] M. L. Ioffredo *et al.*, Paper 37 of Ref. 68.
[75] See p. 120 of Ref. 68.
[76] See Ref. 82.
[77] N. Armenise *et al.*, Phys. Letters **263**, 336 (1968).
[78] A. M. Cnops *et al.*, Paper 210 of Ref. 68.

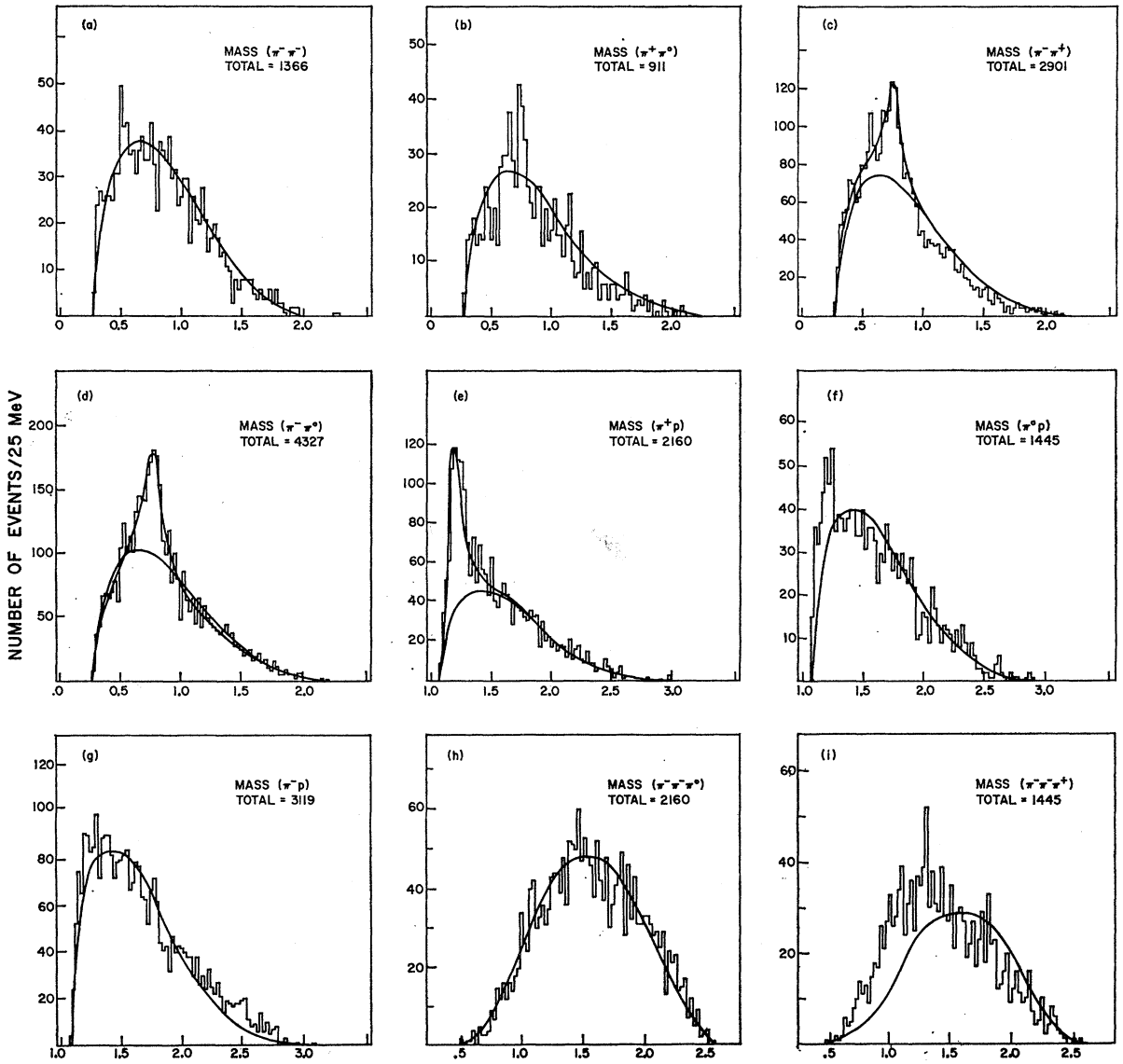

FIG. 7. Invariant-mass distributions for the final state (2). Reflections from dominant resonances are removed (Ref. 93) .The solid curves represent BW fits with phase-space background.

III. FINAL STATES $\pi^-\pi^-\pi^+\pi^0 p$ AND $\pi^-\pi^-\pi^+\pi^+ n$

In this section, we present the results from final states (2) and (3) together. The reason for doing this is based on the observation that the two reactions go through similar intermediate processes and they are often complementary to each other. The first evidence for this observation comes from the invariant-mass distributions shown in Figs. 7–9. It is found that all invariant-mass spectra in both final states are adequately explained by the coherent sum of phase space and resonant amplitudes. If the nonresonant background is indeed approximated by the statistical model, then one can compute the ratio $\sigma(\pi^- p \to \pi^-\pi^-\pi^+\pi^0 p)/\sigma(\pi^- p \to \pi^-\pi^-\pi^+\pi^+ n)$ from the principle of isospin conservation only. The experimental ratio $1.2_{-0.8}^{+1.6}$ obtained after subtraction of resonance productions from each final state is compared to 1.7 obtained from the theoretical calculation.[24] Because of the large uncertainty of the estimation in resonance cross sections, this may not present a very crucial test for the statistical model, but the experimental value is certainly consistent with the hypothesis.

Additional evidence is seen in the angular distributions for outgoing particles measured with respect to the incident pion direction in the over-all center-or-mass system (see Figs. 10 and 11).

The angular distributions for π^-, π^+, and p from the final state (2) can be very well superimposed on those for π^-, π^+, and n from the final state (3). The entire sample, resonances as well as nonresonant scatterings,

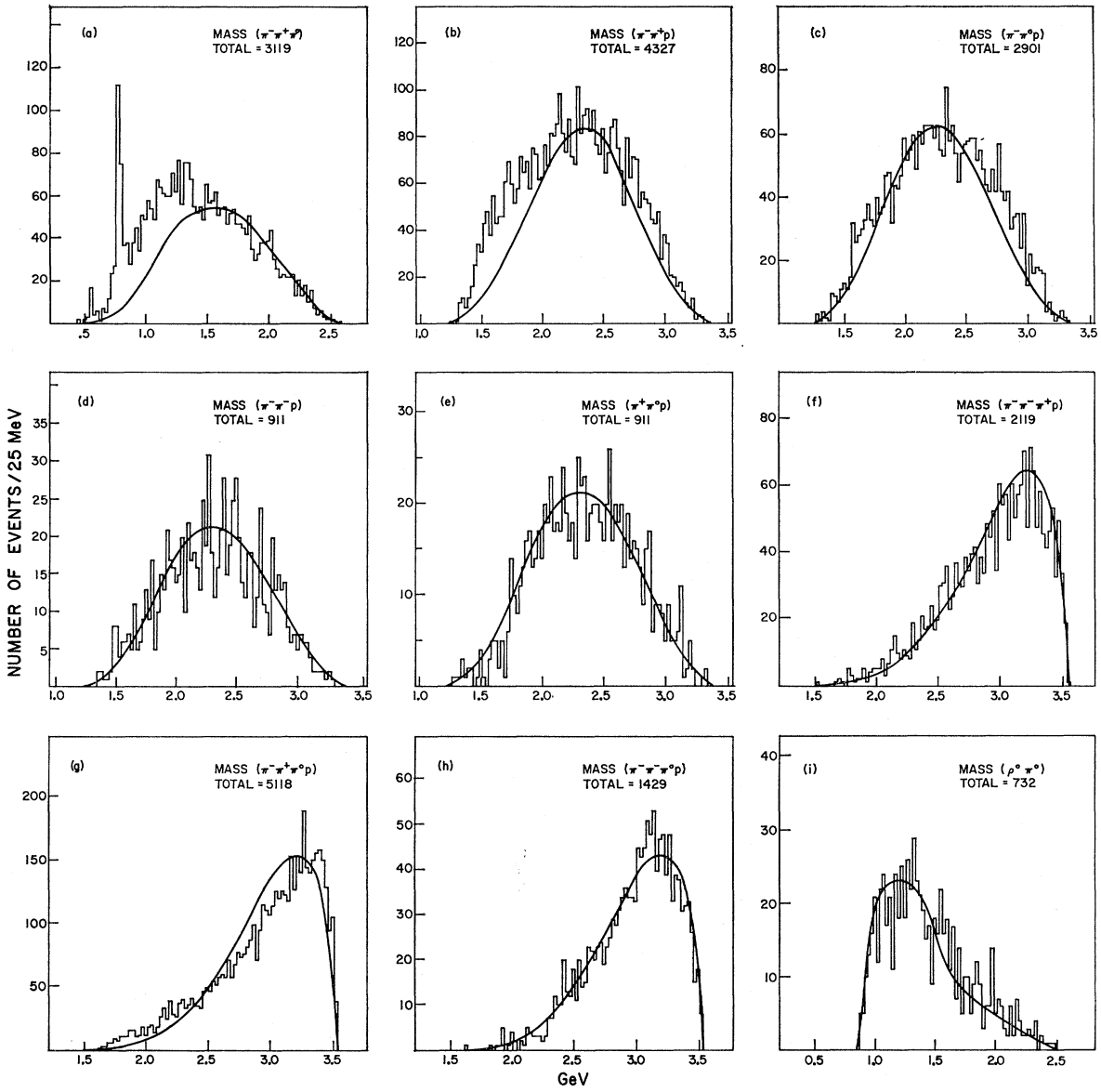

FIG. 8. (a)–(h) Additional invariant-mass distributions (Ref. 93) for the final state (2). The solid curves represent phase space. (i) $M(\pi^0\rho^0)$ distributions with the ρ^- excluded. The solid curve represents the $M(\pi^-\rho^-)$ distribution.

is included in the histograms. This may suggest that the mechanism for resonance productions is also quite similar in both reactions. Obviously, the angular correlations from resonance decays must be taken into account in order to compare the distributions for the scattering angles from two final states. However, the effects coming from the resonance decays may approximately cancel, since resonance productions are dominated by the ρ meson and the $\Delta(1236)$ baryon with roughly the same strength in both final states (see Table VI). The complementary nature of the two final states is then used conveniently for discussing the isospins of various resonance states as well as the appropriate background estimations. For example, in studying A mesons in the $\rho^0\pi^+$ mass distribution, the background may be more properly approximately by the $\rho^-\pi^-$ mass spectrum (at least in the A-meson region), since in this mass spectrum A mesons do not show up because $I^G=1^-$.

The other important resonances produced in the five-body final states are ω^0 and η^0. The relative strengths of production of these resonances are shown in Table VI, together with possible double-resonance productions. The upper limit for the ρ^+ production cross section is approximately 45 μb. This low yield of ρ^+ is observed also in other experiments.[7,12] The ρ^0 production cross sections seem to be also a little smaller than those of the ρ^-. If we assume that ρ mesons are in fact produced

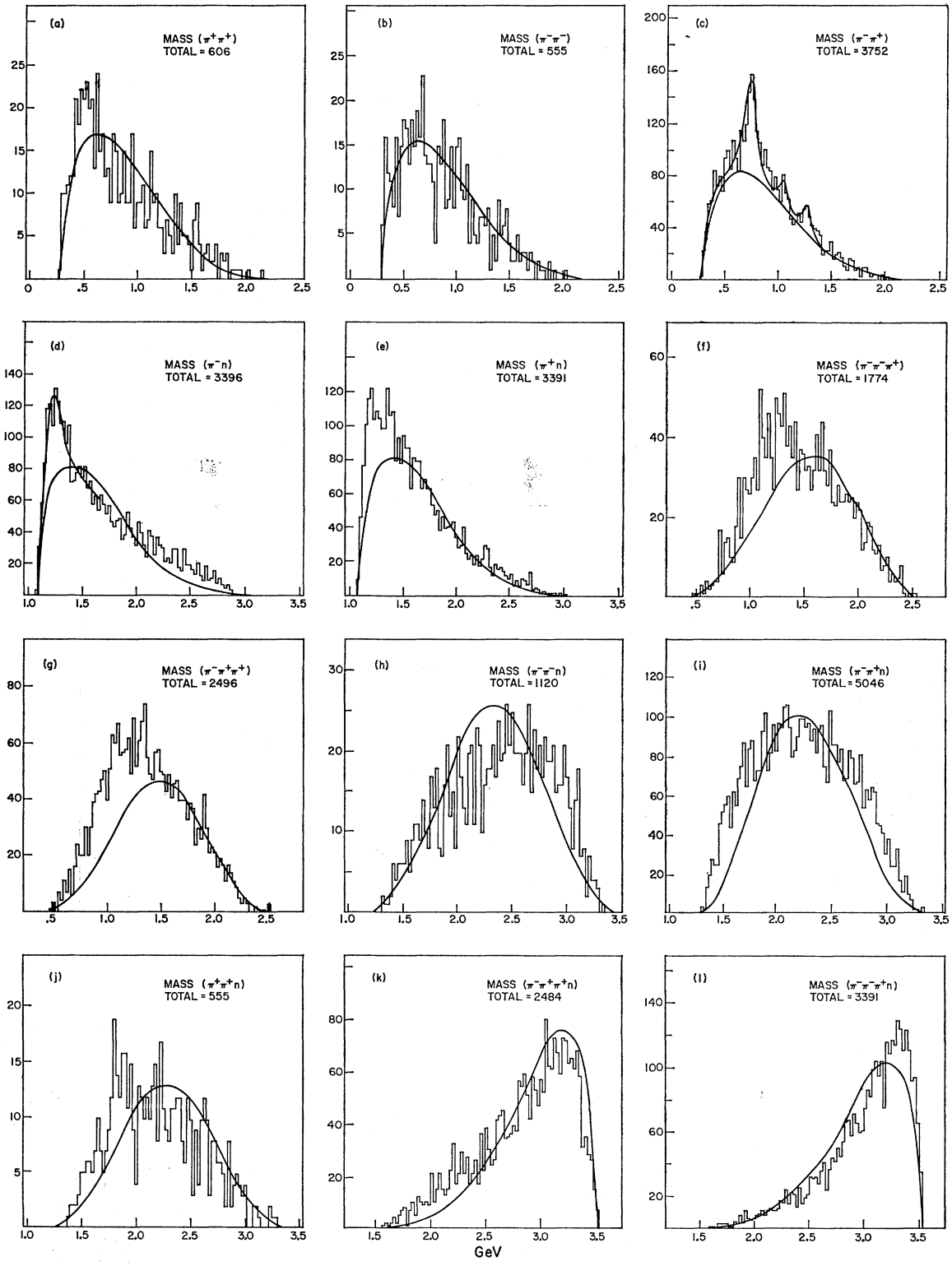

FIG. 9. Invariant-mass distributions for the final state (3). Reflections from dominant resonances are removed (Ref. 93). The solid curves represent BW fits with phase-space background.

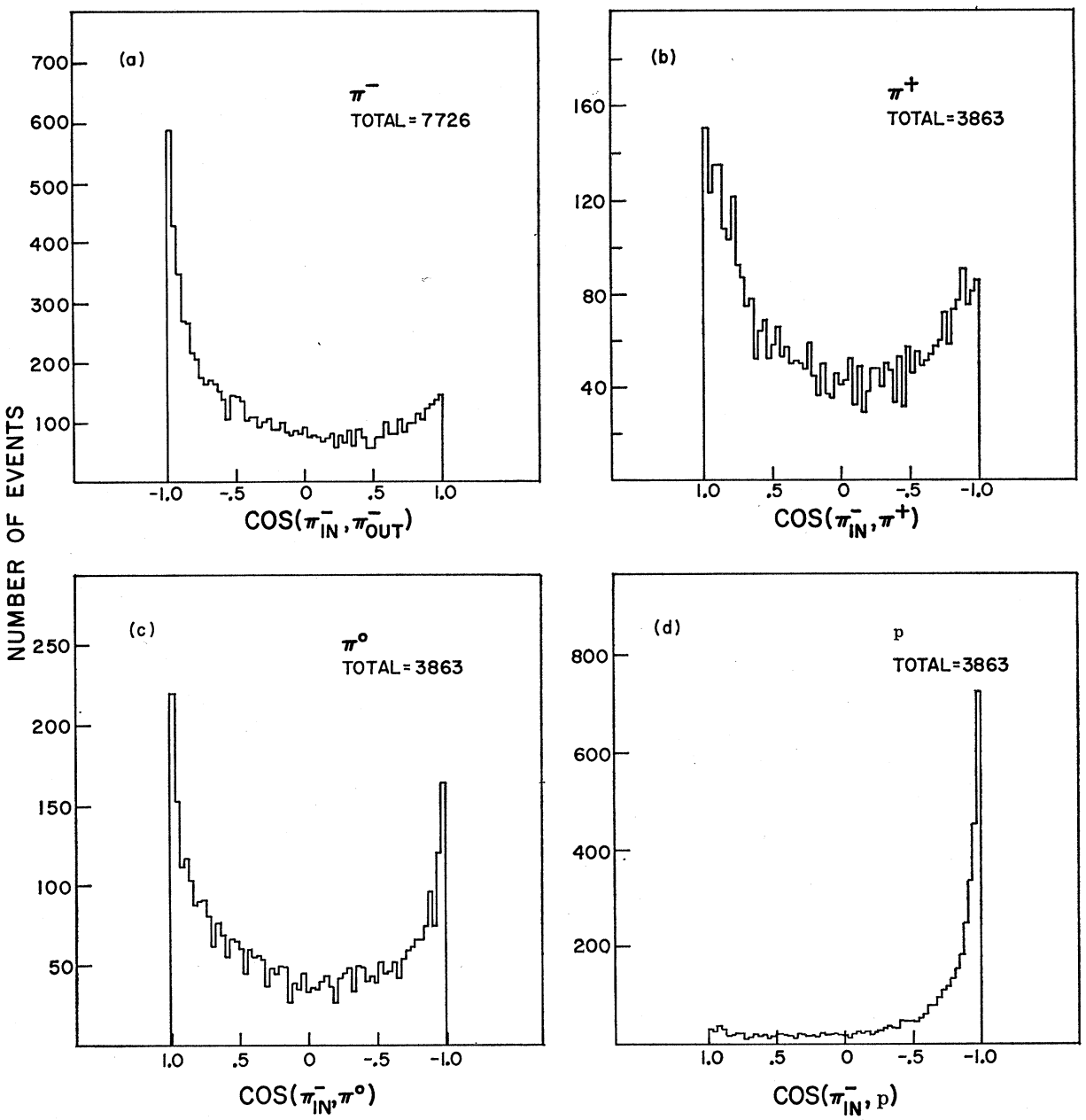

FIG. 10. Angular distributions for outgoing particles in the over-all center-of-mass system from the final state (2). In Fig. 10(a) the abscissa should be labeled $-\cos(\pi_{in}^-, \pi_{out}^-)$.

from the π^- vertex, the absence of doubly charged meson trajectories which couple to the $(\pi^-\rho)$ vertex would prohibit ρ^+ production.

However, if one assumes the multi-Regge-pole model together with the hypothesis proposed by Chew and Pignotti,[79] it would be very hard to suppress ρ^+ production, since in this hypothesis the explicit resonance production diagrams are ignored and only stable particles are included as outgoing particles. A somewhat contradictory situation, however, is observed in $\Delta^-(1236)$ production. Since large momentum transfer from p to $\Delta^-(1236)$ is strongly suppressed (the momentum-transfer distribution is not shown), it may be appropriate to assume nucleon isobar production at the proton vertex. The absence of doubly charged meson trajectories then would prohibit this production just as for the ρ^+. The abundant production of $\Delta^-(1236)$ favors the Chew-Pignotti hypothesis. The sharp peaks observed in the scattering-angle distributions which are not explained by the statistical model may

[79] G. F. Chew and A. Pignotti, Phys. Rev. Letters **20**, 1078 (1968).

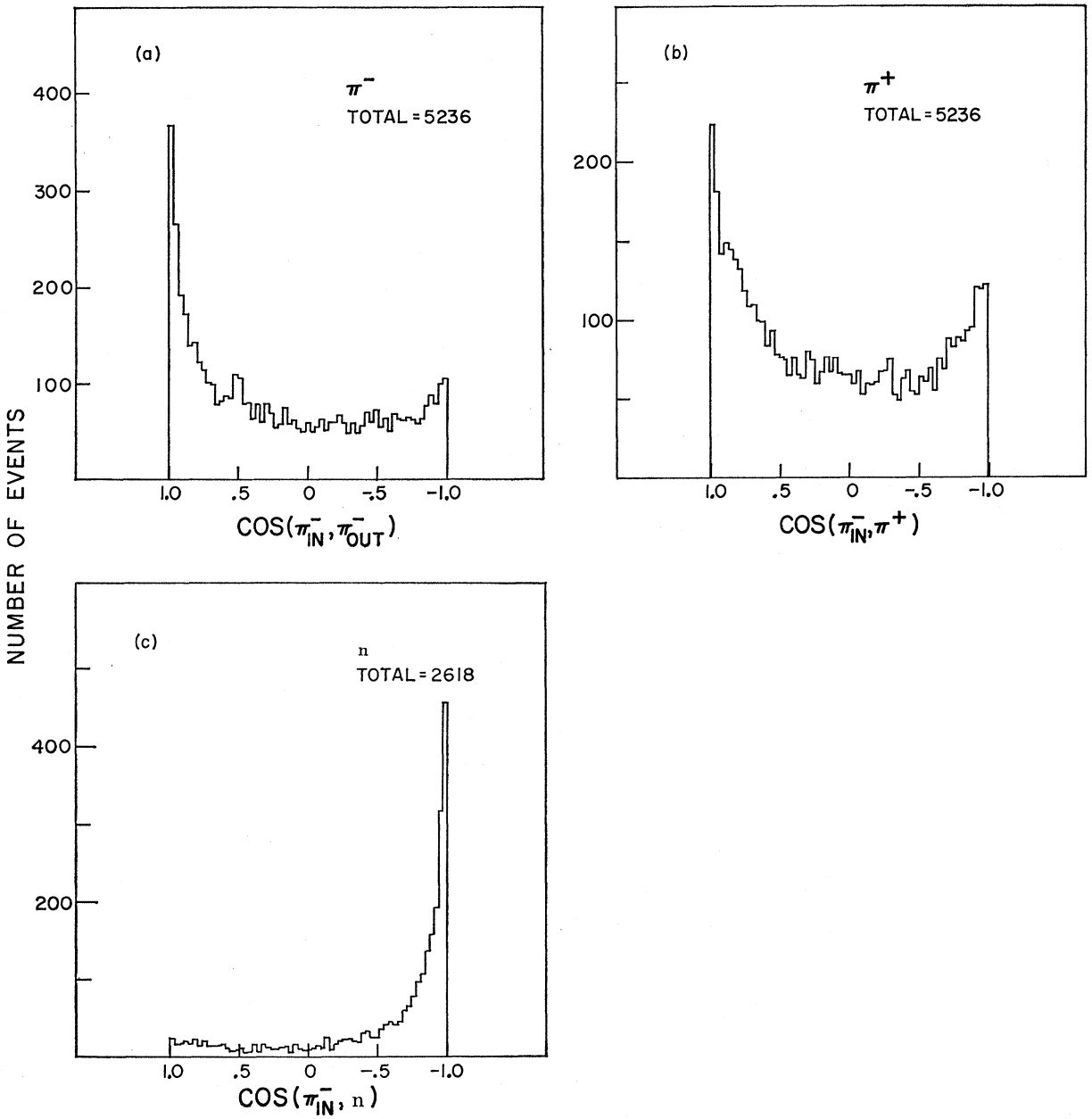

FIG. 11. Angular distributions for outgoing particles in the over-all center-of-mass system from the final state (3).

result naturally from the sum of many peripheral diagrams.

A. Reactions $\pi^- p \to \rho\pi\pi N$

Best values for the ρ parameters as well as cross sections are obtained by Breit-Wigner (BW) fits to the dipion mass spectra:

$$\pi^- p \to \rho^- \pi^- \pi^+ p, \quad 305 \pm 60\ \mu\text{b}; \tag{3.1}$$

$$\to \rho^0 \pi^- \pi^0 p, \quad 260 \pm 54\ \mu\text{b}; \tag{3.2}$$

$$\to \rho^0 \pi^- \pi^+ n, \quad 415 \pm 72\ \mu\text{b}. \tag{3.3}$$

The resonance parameters are given in Table VII. In obtaining the resonance parameters, phase space is assumed as background. Thus the values for the parameters may be a good test for the resonance model.

TABLE VII. Resonance parameters for ρ mesons.

	ρ^-	ρ^0
Mass (MeV)	767±7	756±9
Width (MeV)	165±23	105±40

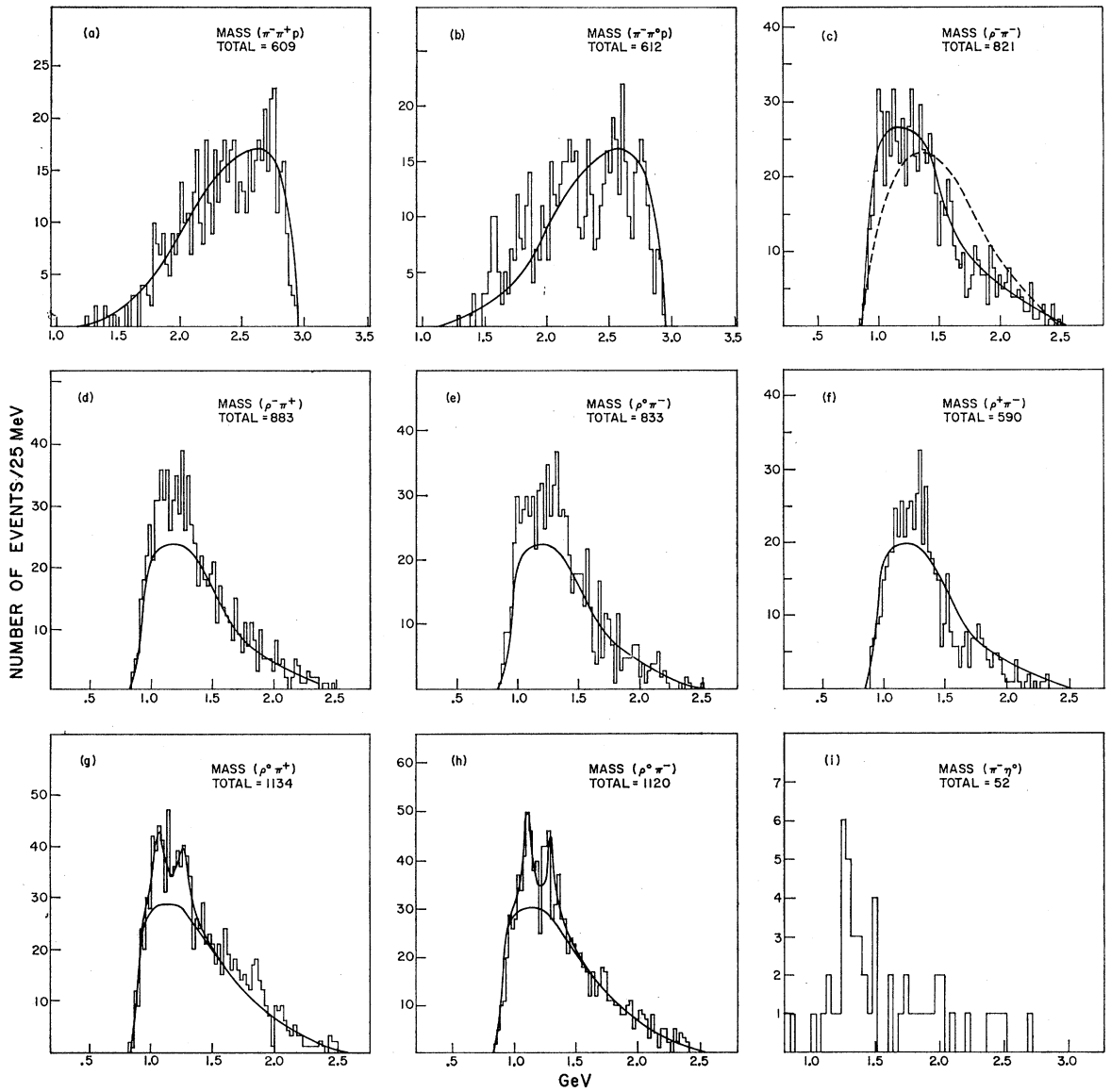

FIG. 12. (a), (b) $M(\pi\pi p)$ distributions with rest of the pions in the ρ. (c)–(h) $M(\pi\rho)$ distributions. The solid curves represent the $M(\pi^-\rho^-)$ distribution. The dashed curve represents $\pi\rho$ phase space. (i) $M(\pi^-\eta^0)$ distribution.

The model seems to describe the invariant-mass distributions adequately.

The cross sections are independently obtained by using the uncut mass distributions with the assumed background interpolated from control regions above and below the resonance region.

Investigations of the possible ρ-N^* associated productions were made to study the meson mass structures in the above-mentioned three channels, since they would complicate the mass distributions and need to be subtracted. Very little evidence is found for two-body modes of formation [see Figs. 12(a) and 12(b)], although clear indications are seen for the three-body intermediate states:

$$\pi^-p \rightarrow \rho^-\pi^-\Delta^{++}(1236), \quad 45\pm20\ \mu\text{b}; \tag{3.4}$$

$$\rightarrow \rho^0\pi^+\Delta^-(1236), \quad 50\pm24\ \mu\text{b}; \tag{3.5}$$

$$\rightarrow \rho^0\pi^-\Delta^+(1236), \quad 36\pm15\ \mu\text{b}. \tag{3.6}$$

The cross sections are compared with those computed from the pure statistical coincidence of the independent ρ and $\Delta(1236)$ productions. No significant deviations from the computed cross sections are observed, indicating that the ρ and $\Delta(1236)$ productions are independent of each other with a very small overlap.

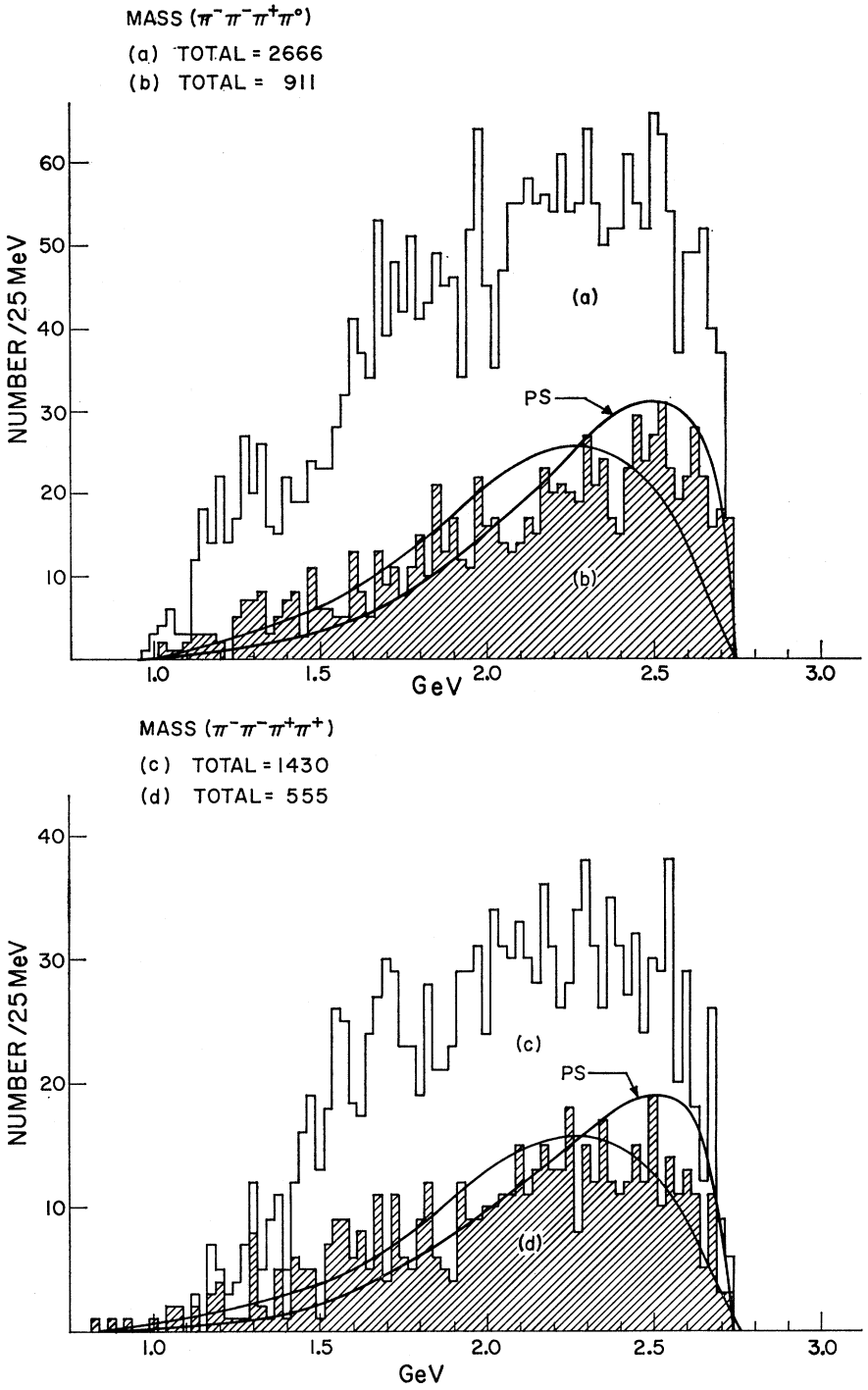

FIG. 13. $M^-(4\pi)$ distributions, (a) excluding $\Delta^{++}(1236)$ and (b) excluding ω^0 and ρ's. $M^0(4\pi)$ distributions, (c) excluding $\Delta^-(1236)$ and (d) excluding ρ^0's.

1. $\rho\pi$ Mass Distribution and A Mesons

The $\rho\pi$ mass spectra are shown in Figs. 12(c)–12(h), with the solid curve representing the nonresonant background. The effect of the Deck mechanism may be most clearly seen in $M(\rho^-\pi^-)$. The reaction (3.1) would proceed via two single-pion-exchange diagrams; since the π^- is scattered forward stronger than the π^+ (as seen in Fig. 10), the kinematic enhancement in the lower-mass region may be larger in $M(\rho^-\pi^-)$ than in $M(\pi^+\rho^-)$.[80]

Phase space [dashed curve in Fig. 12(c)] is compared with the actual $\rho^-\pi^-$ mass spectrum; the deviation from phase space is obvious. Since resonances with $I=1$

[80] S. D. Drell, Rev. Mod. Phys. **33**, 458 (1961).

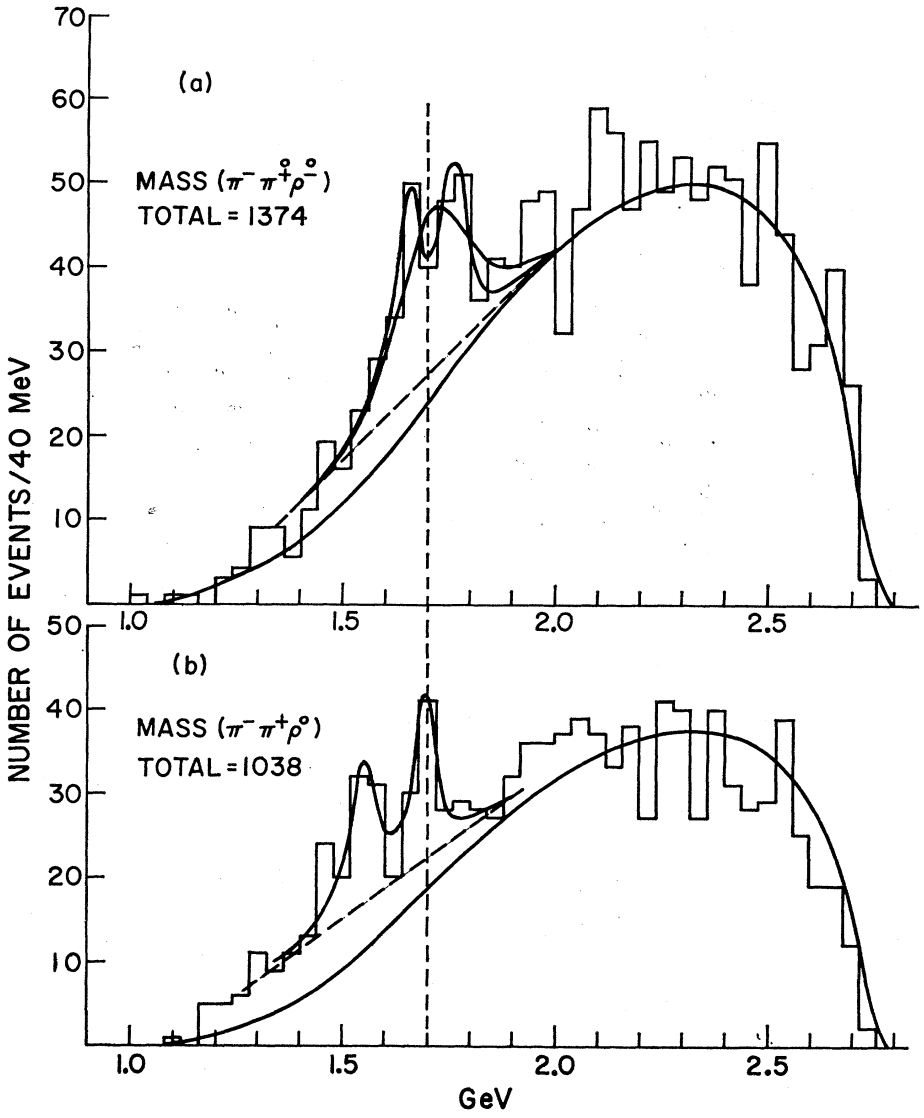

FIG. 14. $M(\pi\pi\rho)$ distributions. The solid curves represent background described in the text.

cannot show up here, this distribution may represent a more realistic background for $I=1$ states. Enhancement of the data appears above this background in Figs. 12(d)–12(h). Assuming that this is caused by A-meson production, we attempted BW fits to $M(\pi^-\rho^0)$ and $M(\pi^+\rho^0)$ where enhancement seems to be more clear. The best fits to these two mass distributions give $M=1096\pm27$ MeV, $\Gamma=90\pm57$ MeV for the A_1 and $M=1295\pm20$ MeV, $\Gamma=102\pm80$ MeV for the A_2, in good agreement with the result from the previous section.

The $\pi^-\eta^0$ decay mode of the A_2 is also seen in Fig. 11(i). The peak falls right at the position where the world-compilation mass spectrum peaks,[68] but in neither is the fine structure of the A_2 seen.

Since the "death" of the H meson at 990 MeV,[68] the search for the missing isoscalar member of the $J^{PC}=1^{+-}$ nonet has continued but no candidate has been found yet. We examined the $\rho^0\pi^0$ mass spectrum from the suggestion by Harari[81] and see no evidence for the missing isoscalar [see Fig. 8(i)]. In fact, the mass spectrum looks just like $M(\rho^-\pi^-)$, which is drawn as the solid curve in this figure.

2. $\rho\pi\pi$ Mass Enhancements

The 4π mass distributions with $\Delta(1236)$ excluded are shown in Fig. 13. A large deviation from 4π phase space is observed. This is due in part to the strong ρ and ω^0 production and in part to peripheral scattering. In fact, elimination of ω^0 and η^0 associated events

[81] H. Harari, in *Proceedings of the Fourteenth International Conference on High-Energy Physics, Vienna, 1968*, edited by J. Prentki and J. Steinberger (CERN, Geneva, 1968), p. 195.

removes the low-mass enhancements in $M^-(4\pi)$ which are completely absent in $M^0(4\pi)$. Further elimination of ρ mesons leaves $M(4\pi)$ essentially structureless, although still not consistent with phase space [see Figs. 13(b) and 13(d)]. The fit is somewhat improved if we use peripheralized phase space. A factor $e^{\alpha t}$, where t is the usual four-momentum transfer to the nucleon, is included. The result with $\alpha=3.0$ GeV^{-2} is shown together with pure phase space. The fit seems to be adequate with $\alpha\sim 2.0$ GeV^{-2} for both charged states.

The parameter α can be obtained independently from the actual four-momentum distributions for the nucleon, and is found to be consistent with the value required for the peripheralization.

The $\rho\pi\pi$ mass spectra are shown in Fig. 14. The over-all shape of the distributions is compared with the incoherent sum of three phase-space distributions: 40% 4π, 43% $\rho\pi\pi$, and 17% $\rho\rho$. The effect of peripheral scatterings is included only in the 4π phase space and ignored in other channels. The low-mass enhancements are clear. In the following, we consider first the possibility of two peaks, one at 1650 and the other at 1750 MeV in $M^-(\rho\pi\pi)$. The enhancement around 1550 MeV in $M^0(\rho\pi\pi)$ may correspond to an $I=0$ state, since this enhancement does not show up in $M^-(\rho\pi\pi)$.

The phase-space prediction for masses below the two enhancements in each charged state is inconsistent with the data. Therefore, we assume the background in the resonance regions to be linearly interpolated from the adjacent regions. The best estimates of the resonance parameters, assuming two peaks in the $M^0(4\pi)$, are $M=1549\pm16$ MeV, $\Gamma=72\pm47$ MeV for the first peak and $M=1690\pm19$ MeV, $\Gamma=37_{-37}{}^{+64}$ MeV for the second peak. Similar fits to a double peak in $M^-(4\pi)$ are obtained with $M=1676\pm17$ MeV, $\Gamma=77\pm40$ MeV and $M=1780\pm7$ MeV, $\Gamma=42_{-42}{}^{+86}$ MeV.

It may also be the case that there is just a single peak, even though the resolution of our experiment (8 ± 3 MeV) is sufficient to differentiate peaks separated by the order of 100 MeV. An equally good fit to one peak is obtained with $M=1716\pm22$ MeV, $\Gamma=203\pm89$ MeV. (Confidence levels are 50 and 43% for the double peak and single peak, respectively.)

There have been many experiments reported[82] on the evidence for $I=1$ enhancements in this energy region. The missing-mass experiment[83] has seen three peaks at 1630, 1700, and 1750 MeV with widths less than 15 MeV, which we will tentatively call R_1, R_2, and R_3, respectively. Because of the small widths of these bumps, we prefer a double-peak assumption in the $M^-(4\pi)$ spectrum. The agreement in the mass and width in the different charged states then becomes quite good:

$$M(R_2^-)=1676\pm17 \text{ MeV}, \quad \Gamma(R_2^-)=77\pm40 \text{ MeV};$$
$$M(R_2^0)=1690\pm19 \text{ MeV}, \quad \Gamma(R_2^0)=37_{-37}{}^{+64} \text{ MeV}.$$

The 1780 ± 17-MeV peak may correspond to this R_3 peak in our data. The mass and width are in relatively good agreement with the missing-mass experiment, but the corresponding $I_z=0$ state is not observed in the $M^0(4\pi)$. This is difficult to understand unless the R_3 bump decays mainly into $\rho\rho$, since $R_3^0\to\rho^0\rho^0$ is prohibited from isospin conservation. The R_3 peak, however, disappears in the $\rho\rho$ mass distributions (see Fig. 15), and the remaining peak must be the R_2^-.

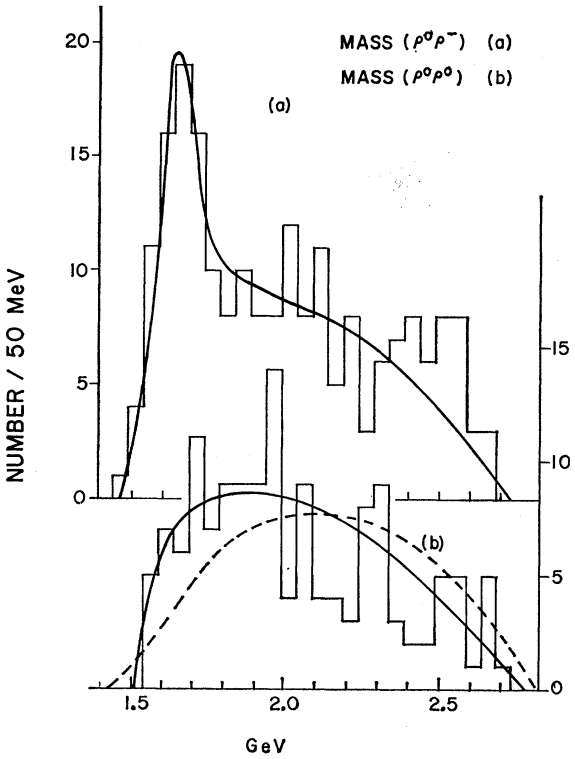

FIG. 15. $M(\rho\rho)$ distributions. The dashed curve represents phase space.

TABLE VIII. Charged "g" meson.

Ref.	Reaction	Beam momentum (GeV/c)	M (MeV)	Γ (MeV)	$g^-\to\pi^-\pi^0$ (μb)	$g^-\to\rho^-\rho^0$ (μb)
Crennel *et al.* (84)	π^-p	6.0	1630	200	40±20	no data
This expt.	π^-p	6.7	1640±20	129±66	no data	≥24
Johnston *et al.* (15)	π^-p	7.0	1675±10	90±0	35	33
Biswas *et al.* (17)	π^-p	8.0	1710±23	$162_{-40}{}^{+58}$	18	60±20
Caso *et al.* (85)	π^-p	11.0	1670–1720	100–120	no data	40–60
Ballam *et al.* (19)	π^-p	16.0	1700±35	180±50	no data	30±10

[82] See Ref. 15, 17, 19, 83, and 84. See also T. Ferbel, in *Meson Spectroscopy*, edited by C. Baltay and A. H. Rosenfeld (W. A. Benjamin, Inc., New York, 1968), p. 335.

[83] L. Dubal *et al.*, Nucl. Phys. **B3**, 435 (1967).

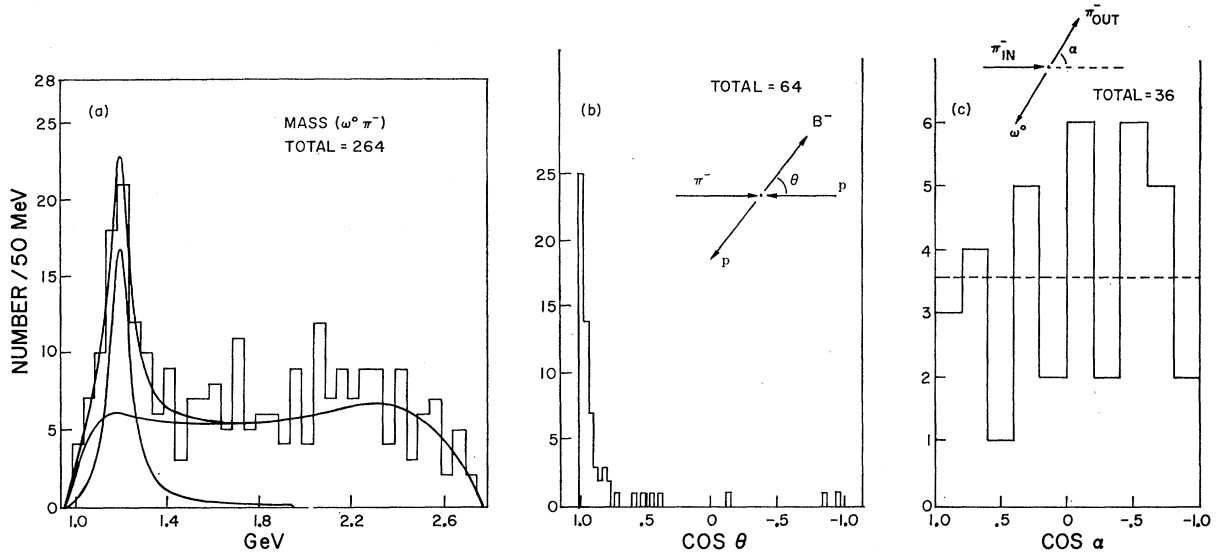

FIG. 16. (a) $M(\pi^-\omega^0)$ distribution. (b) Scattering-angle distribution for the B. (c) Decay angular distribution.

Since this peak comes at the threshold of the $\rho^-\rho^0$ mass distribution, the background estimation is difficult. One can however, argue that the effect of kinematical enhancements in the $\rho^0\rho^-$ mass spectrum is less than or equal to that in the $\rho^0\rho^0$ spectrum; thus the background in the $M(\rho^-\rho^0)$ may be approximated by $\rho^0\rho^0$, as was first discussed by Biswas *et al.*[17] If we assume this background, then the $\rho^0\rho^-$ mass enhancement becomes clear. The best estimates for mass and width are compared with the other bubble-chamber experiments in Table VIII.[84,85] Since there is no enhancement in $\rho^0\rho^0$, the isospin of the R_2 may very well be unity. Furthermore, $R_2^- \to \rho^-\rho^0$ is the dominant decay mode. Since the neutral state is forbidden to decay into $\rho^0\rho^0$, $\rho\pi\pi$ and 4π decay modes are important. These features are all consistent with the resonance interpretation of the R_2 enhancement, but it is still difficult to understand why there is no enhancement around 1750 MeV in the $M^0(4\pi)$. We can make an assumption on the production mechanism of the peak by some isoscalar exchange such as ω^0, for example, which would prohibit the production of the zero-charged state. Unfortunately, test of this assumption is impeded by the unknown absorption corrections (or the unknown residue function for the ω^0 trajectory). The Treiman-Yang angle was also examined in this mass region to see if ω^0 exchange is possible. An approximately flat distribution was obtained, indicating that pion exchange cannot be excluded.

On the other hand, if one takes the single-peak assumption, the large discrepancy in the observed widths between the two charged states of the 1700-MeV peak is difficult to understand. One possible explanation involves the different decay widths for the $\rho\rho$ and $\rho\pi\pi$ decays and the interference between them. Since interference is absent in the zero-charged state, the observed value of approximately 30 MeV may be appropriate for the $\rho\pi\pi$ width. Assuming the same mass for the different decays, we obtained a fit to the data with confidence level of 25% by two BW amplitudes with destructive interference: $M=1704\pm22$ MeV, $\Gamma_{\rho\rho}=140$ MeV, and $\Gamma_{\rho\pi\pi}=30$ MeV. If we further assume a slightly different mass for each decay, the fit would improve.[86] Since the parametrization is not unique, we conclude that the interference model is equally probable at this statistical level.

The bump at 1548 ± 16 MeV in the $I=0$ state is of some interest. The observed signal is a 4-standard-deviation effect. Together with the symmetric decay angular distribution, a resonance interpretation is favored. From the observed mass and width, it may be most natural to identify this with $f'(1515)$. Recently, Ascoli *et al.*[82] reported the decay mode $f^0(1250) \to 4\pi$. This evidence was found in the same final state as ours at 5.0 GeV/c. We are not able to give the relative strength of the decay modes $\rho^0\rho^0$, $\rho^0\pi^-\pi^+$, and 4π, but $\rho^0\rho^0$ decay mode is most likely negligible.

3. *Reaction* $\pi^-p \to \pi^-\omega^0p$

The cross section for this reaction is 160 ± 22 μb, which amounts to $\sim$9% of the final state (2). In the $\pi^-\omega^0$ mass distribution (see Fig. 16) a strong B-meson peak is observed. We looked for possible contamination such as ω^0N^*, but no obvious signal is seen. The background is computed by the Monte Carlo method. This

[84] D. J. Crennell *et al.*, Phys. Rev. Letters **18**, 323 (1967).
[85] C. Caso *et al.*, Nuovo Cimento **47A** 675 (1967); **51A**, 175 (1967).

[86] The simplest possible form, background $[\alpha+\beta(\mathrm{BW}_1+\gamma\mathrm{BW}_2)^2]$, was used for the fit, where $\mathrm{BW}_i=(\Gamma_i/2)^2/[(M-M_0)^2+(\Gamma_i/2)^2]$.

reproduces the general features of the $\pi^-\omega^0$ mass distribution quite well. The BW distribution fitted to the data gives $M=1200\pm15$ MeV and $\Gamma=113\pm44$ MeV for the mass and width of the B, respectively. These parameters are compared with other experiments and summarized in Table IX.[87-92] The t dependence of the production cross section is fitted to e^{at} with $a=5.5\pm2.5$ GeV^{-2}, which may be compared to ~4 GeV^{-2} at 5.0 GeV/c obtained by Ascoli *et al.*[10] The sharpness of the forward peak in the scattering-angle distribution [Fig. 16(b)] led us to study the spin and parity by the Adair method. The decay angle α shown in Fig. 16(c) between the incident pion and the decay pion not in the ω^0 in the B system is used to examine the relative orbital angular momentum (events are taken when $\cos\theta\geq0.95$). $J^P=0^+$, 0^-, 1^-, 1^+, 2^+, and 2^- are tried with arbitrary parameters for the spin-flip amplitudes as well as the mixing of two orbital angular momenta. Because of these free parameters, the result is equally good for all assumptions and we are not able to discriminate among them.

TABLE IX. B meson.

Ref.	Reaction	Momentum (GeV/c)	M (MeV)	Γ (MeV)	$\sigma(B\to\omega^0\pi^-)$ (μb)
Abolins *et al.* (89)	π^+p	3.5	1220	100±20	115+30
Goldhaber *et al.* (90)	π^+p	3.65	1220	80	85±35
Chung *et al.* (91)	π^-p	3.2	1220±20	150±20	109±30
	π^-p	4.2			67±20
This expt.	π^-p	6.7	1200±15	113±44	25±10
ABC (15)	π^+p	8.0	1259±27	204±75	28±9
Caso *et al.* (85)	π^-p	11.0	1250		30
Ballam *et al.* (19)	π^-p	16.0	1250±35	200±50	25_{-10}^{+20}
Baltay *et al.* (92)	$\bar{p}p$	rest	1200±20	100±50	

IV. SUMMARY

All three final states $\pi^-\pi^-\pi^+p$, $\pi^-\pi^-\pi^+\pi^0p$, and $\pi^-\pi^-\pi^+\pi^+n$ are mediated by a variety of resonance production processes which amount to more than 50% of the total events.[93] ρ mesons and $\Delta(1246)$ are most copiously produced, while the higher boson and nucleon resonances such as $A_1(1100)$, $A_2(1300)$, $R(1640)$, $\rho(1700)$, $N(1518)$, and $N(1690)$ are found to have large branching ratios for decay into the lower resonance states. Both $\pi\rho$ and $\pi\eta$ decay modes for $A_2(1300)$ are observed with no double-peak structure. There is evidence for resonance behavior of $A_1(1100)$, and the J^P assignment for the A_1 is consistent with 1^+. The clear signal for $A_{1.5}(1200)$ comes only from the final state $\pi^-\pi^-\pi^+p$. The spin-parity analysis rules out 0^- and 2^+ for the $A_{1.5}$. Enhancements are observed in the R-meson region in the 3π and 4π invariant-mass distributions. The signals are enhanced when $f^0(1250)$ and $\rho(760)$ are required in the 3π and 4π mass distributions, respectively. The $f^0\pi^-$ enhancement appears at 1633±12 MeV with width 37±24 MeV. The 4π enhancements in this mass region appear to be more complicated. In the zero-charged state, two enhancements at 1549±16 and 1690±19 MeV are observed, of which the former enhancement may correspond to $f'(1515)$. Corresponding to the enhancement at 1690 MeV, in the negative-charged state we observed a peak at 1676±17 MeV, which seems to decay dominantly into $\rho^0\rho^-$. In the negative-charged state there seems to be another peak at 1780±7 MeV, which has no corresponding enhancement in the zero-charged state. At the present statistical level we may also assume a single peak at 1716±22 MeV with width of 203±89 MeV. The interference between the $\rho\pi\pi$ and $\rho\rho$ decay modes of the same peak at $\sim$1700 MeV is possible. A strong B meson is observed in the $\pi^-\omega^0$ mass distribution. Peripherality of the background is stronger in final state (1) than in the other final states.

[87] The angular distributions between the incident pion and the decaying ρ^0 in the rest frame of the 4π mass are examined at several masses, including the mass band which includes the 1549-MeV peak. The result (not shown) seems to support the resonance interpretation of the peak. Since the mixing of two decay modes $\rho\pi\pi$ and of 4π is difficult to obtain, the further analysis of the spin and parity of the peak was not attempted.

[88] G. Ascoli, H. B. Crawley, D. W. Mortara, and A. Shapiro, Phys. Rev. Letters **21**, 1712 (1968).

[89] M. Abolins, R. L. Lander, W. A. W. Mehlhop, N. H. Xuong, and P. M. Yager, Phys. Rev. Letters **11**, 381 (1963).

[90] G. Goldhaber, S. Goldhaber, J. A. Kadyk, and B. C. Shen, Phys. Rev. Letters **15**, 118 (1965).

[91] S. U. Chung *et al.*, Phys. Rev. Letters **16**, 481 (1966).

[92] C. Baltay, J. C. Severiens, N. Yeh, and D. Zanello, Phys. Rev. Letters **20**, 1411 (1968).

[93] Dominant resonances ρ, ω^0, $\Delta^{++}(1236)$, and $\Delta^-(1236)$ are removed whenever one or more particles in the invariant-mass combinations form the above resonances together with particles outside the combinations: ρ cut, 660–860 MeV; ω^0 cut, 730–830 MeV; and Δ^{++} and Δ^- cuts, 1136–1336 MeV.